



Royal Netherlands  
Meteorological Institute  
Ministry of Infrastructure and the  
Environment

The EUMETSAT  
Network of  
Satellite Application  
Facilities



**OSI SAF**  
Ocean and Sea Ice



**EUMETSAT**

## Ocean and Sea Ice SAF

# ASCAT NWP Ocean Calibration

**Jeroen Verspeek  
Anton Verhoef  
Ad Stoffelen**

**Version 1.5**

**2011-03-16**

# Contents

1	Introduction .....	3
2	NWP Ocean Calibration.....	3
3	Derivation of the NOC correction factors .....	5
4	Verification of the NOC correction factors .....	12
5	ASCAT stability .....	15
6	Visualisation .....	18
7	MLE normalisation and QC .....	22
8	Effects of NOC and new QC tables.....	26
8.1	Wind statistics .....	26
8.2	Quality flags .....	29
8.3	MLE distribution .....	29
9	Conclusions .....	31
	Annex – .....	33
	Tuning of AWDP MLE normalisation and Quality Control threshold tables.....	33
	General considerations .....	33
	Step 1.....	33
	Step 2.....	34
	Step 3.....	35
	Glossary.....	36
	References .....	36

# 1 Introduction

The objective of Ocean Calibration (OC) is to find corrections of the normalized radar cross section,  $\sigma_0$ , per antenna and Wind Vector Cell (WVC) that improve the ASCAT wind retrieval. The Numerical Weather Prediction (NWP) Satellite Application Facility (SAF) ASCAT Wind Data Processor (AWDP) is used for the ASCAT wind retrieval [NWPSAF site; ASCAT user manual].

Currently, AWDP uses corrections based on a visual correction method for OC (VOC) [Verspeek et al. 2008]. In this method the Geophysical Model Function (GMF) is evaluated in the measurement space for its consistency with the distribution of measurement points. The measurement space is defined for each WVC as the three-dimensional or 3D (x,y,z) space spun up by the measured values of respectively the fore, aft and mid beams [Stoffelen and Anderson, 1997]. The two-dimensional (2D) GMF surface is a conical surface and the (fore, aft, mid) measurement triplets should generally lie in the proximity of this surface. The visual correction method scales the three axes of the measurement space, i.e., the fore, aft and mid beam  $\sigma_0$ s, such that the distribution of measurement triplets is shifted towards the conical GMF surface.

Another method for Ocean Calibration (OC) resides in direct comparison of measured  $\sigma_0$  data with simulated values from NWP winds using the GMF [Stoffelen, 1998; Freilich, 1999; Verspeek, 2006]. For the ASCAT and ERS scatterometers this NWP-based OC (NOC) estimates  $\langle z \rangle$ , the mean transformed backscatter over the ocean for a uniform wind direction distribution and compares this with the mean measured backscatter over the ocean for a given wind distribution, as further explained in section 2.

The VOC and NOC methods each have their pros and cons. In this report we will evaluate these and verify how both VOC and NOC antenna and WVC dependent correction tables improve the wind retrieval. The aspects of the wind retrieval that are most affected by the correction tables are the Quality Control (QC), retrieved wind direction distribution and thus wind direction error and the distribution of normalized distance between measurement triplet and GMF in measurement space. Metrics based on the statistical distribution of these variables will be discussed and evaluated in section 8.

## 2 NWP Ocean Calibration

The NOC technique [Stoffelen 1998] is used to assess the difference between scatterometer backscatter data and simulated backscatter data out of collocated NWP winds using the GMF. Discrepancies between mean measured and simulated backscatter may be due to instrument calibration, systematic and random errors in NWP wind speed and direction and GMF errors. These sources of error should therefore be analyzed carefully. The NOC method is based on the analysis of a large measurement dataset to estimate Fourier coefficients that can be directly compared to those in the CMOD5.n GMF. For any particular WVC in any beam the incidence angle is very nearly constant around the orbit and we can model the backscatter with

$$\sigma_0(v, \phi) = B_0(v) [1 + B_1(v) \cos \phi + B_2(v) \cos(2\phi)]^{1.6}$$

where  $v$  is wind speed and  $\phi$  is wind direction with respect to the beam pointing direction. The mean backscatter is essentially determined by the value of  $B_0$  with contributions from  $B_1$  and  $B_2$ . In  $z$ -space, where  $z = \sigma_0^{0.625}$ , this becomes

$$z(v, \phi) = \frac{1}{2} a_0(v) + a_1(v) \cos \phi + a_2(v) \cos(2\phi)$$

where  $a_0 = 2B_0^{0.625}$ ,  $a_1 = B_1B_0^{0.625}$  and  $a_2 = B_2B_0^{0.625}$ . Integrating uniformly over the azimuth angle gives

$$\frac{1}{2\pi} \int_0^{2\pi} z(v, \phi) d\phi = \frac{1}{2} a_0(v)$$

So, when the wind direction distribution is sampled uniformly for all wind speeds, then the mean of  $2a_0$  should be identical to the mean of  $z$ . This means that uncertainties in  $a_1$  and  $a_2$  do not contribute to the error in the simulated mean  $z$ .

To arrange a uniform wind direction distribution, we split the data into wind speed bins and azimuth angle bins. Bins are defined so that they are large enough to contain a certain minimum number of measurements and small enough to provide a good approximation of the integral. In the following, indices  $i$  and  $j$  refer to wind speed bin  $i$  and azimuth angle bin  $j$  respectively. Index  $k$  is used to refer to an individual measurement  $z_k$ . Parameters  $I$ ,  $J$  and  $K$  refer to the total number of bins or measurements, so  $i=1, 2 \dots, I$ ,  $j=1, 2 \dots, J$  and  $k=1, 2 \dots, K(i,j)$ .

The mean  $z$  in a fixed wind speed row is, let's call this  $z(i)$ :

$$z(i) = \frac{1}{J} \sum_{j=1}^J \frac{1}{K(i,j)} \sum_{k=1}^{K(i,j)} z_k(i,j)$$

Summation over the wind speed rows gives

$$\langle z \rangle = \frac{1}{KJI} \sum_{i=1}^I KJ(i) z(i)$$

with

$$KJ(i) = \sum_{j=1}^J K(i,j), \quad KJI = \sum_{i=1}^I \sum_{j=1}^J K(i,j)$$

$\langle z \rangle$  is the mean backscatter value over a uniform wind direction distribution and may be either measured or simulated by collocated NWP wind inputs and the GMF, where mainly the term as given by  $a_0(v)$  or  $B_0(v)$  contributes. Any discrepancy between the simulated and measured mean backscatter values is computed as a ratio. A ratio not equal to one may be related to inaccuracies in the instrument gain, e.g., beam pattern determination, or to errors in the NWP input winds and GMF.

This method needs only a few days of collocated ASCAT data and ECMWF winds to produce a reasonable estimate of difference in  $a_0$ . We use CMOD5.n with the ECMWF equivalent neutral 10-meter winds to calculate model backscatter values corresponding to the collocated measured values and apply the process as described above. The difference between the two values of  $a_0$  then provides an estimate of the mean difference between model and measurement backscatter.

### 3 Derivation of the NOC correction factors

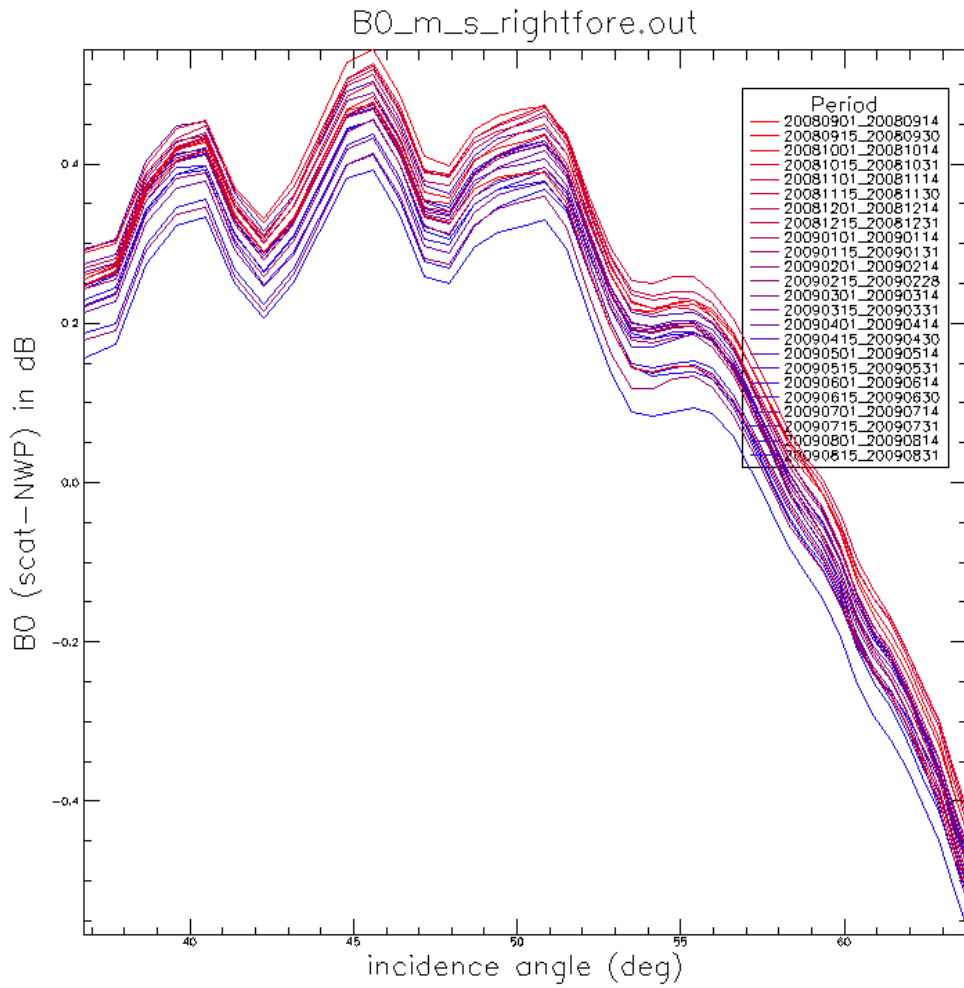
The ocean calibration gives residuals in backscatter as a function of incidence angle for each antenna. When these residuals are stable over time they may be used as correction factors for errors in the instrument, for monitoring instrument health or for GMF development.

A time series of the ocean calibration is performed over the period of one year, from 2008-09-01 to 2009-08-31 for the ASCAT scatterometer in high-resolution mode (12.5 km WVC spacing). The one-year period is taken to average out the seasonal variations in the wind distribution that have an effect on the NOC residual. Successive periods of day 1-14 and day 15-last day of the month are taken as input for an ocean calibration run. The cone corrections [Verspeek et al, 2008] are not applied, but only a correction that accounts for the differences in level1B software processing versions. These corrections have been able to transform the ASCAT backscatter measurements from each L1B calibration cycle to the next cycle within a few hundredths of a dB. L1B software version 7.02 with the 3-transponder calibrated data is taken as the reference. Thus the results are made independent of the level1B software version that is used. For a detailed description of the precision in the correction factors see Verspeek et al [2008].

Figure 1 shows the ocean calibration residuals from the right-fore antenna as a function of incidence angle. Each line corresponds to a time period.

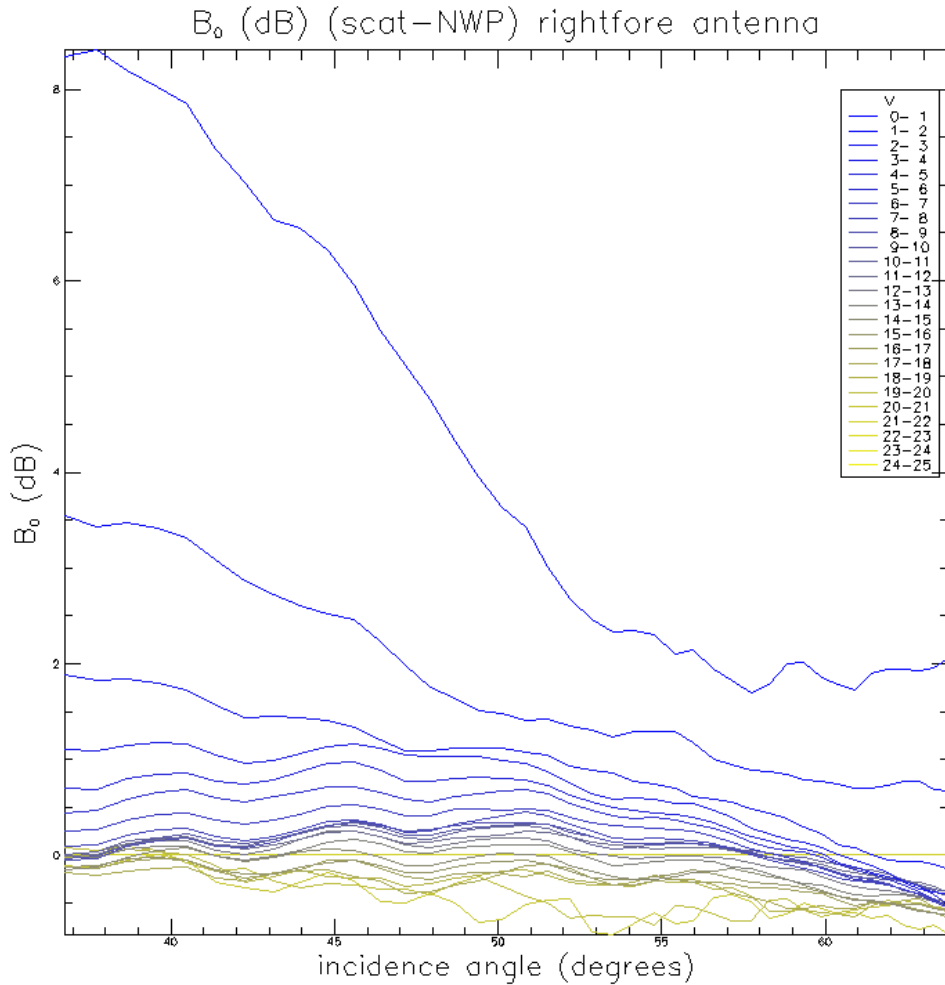
The figure shows a good stability over time with a fluctuation  $\sim 0.1$  dB. Variations in NWP wind distribution over time are the main cause of these fluctuations. However, the latest results appear slightly lower than the earliest with an apparent gradual degradation. It is not clear whether this is due to the ASCAT instrument or to the input NWP winds. Stoffelen [1998] notes that changes in wind speed scaling show an incidence-angle dependent bias, whereas here a rather constant degradation appears over time.

The pattern as a function of incidence angle shows distinct peaks and troughs. These are difficult to explain from the NWP comparison procedure [Stoffelen, 1998] since the GMF terms are rather smooth as a function of incidence angle and subsequent WVCs see almost identical NWP wind distributions. Also for the other antennas the pattern is stable over time, with a similar incidence-angle independent vertical shift over time.



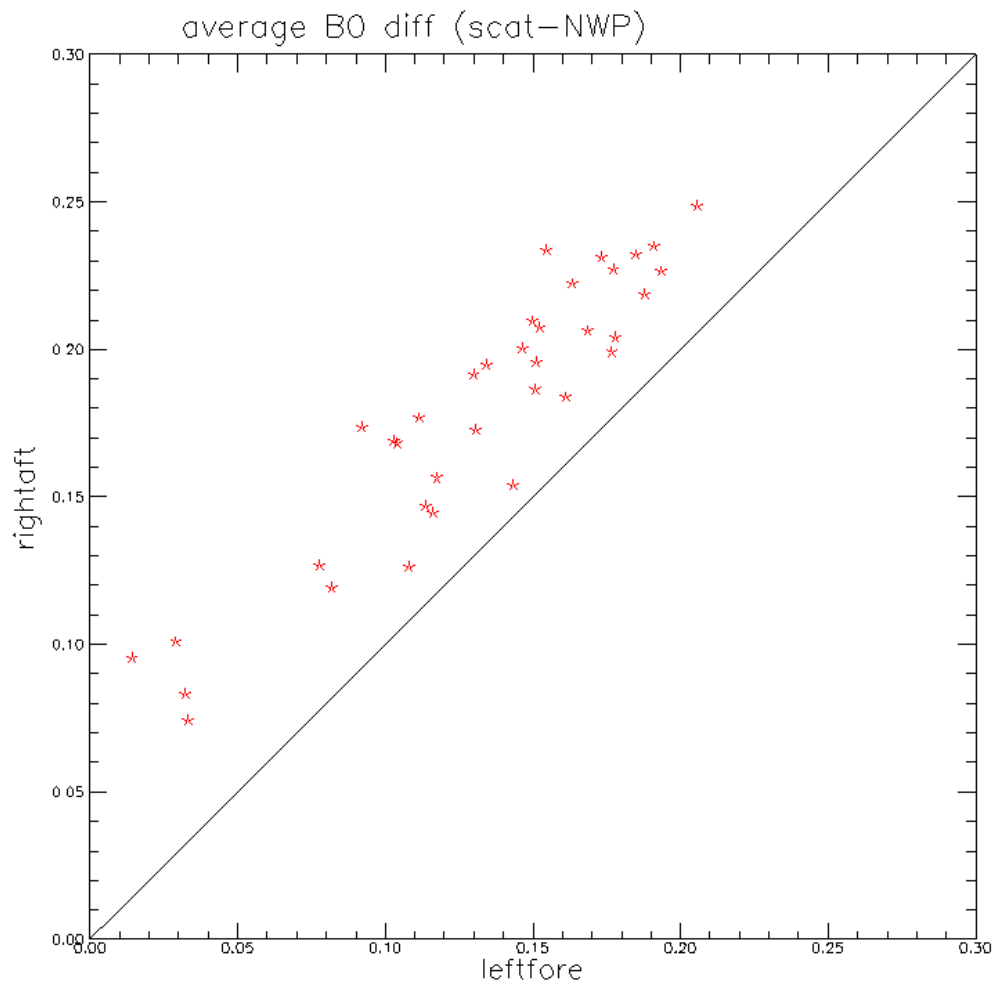
**Figure 1** – Stability over time of the right-fore antenna ocean calibration residual as a function of incidence angle.

Figure 2 shows a typical example of the  $B_0$  residual for the right-fore antenna per wind speed bin. These residuals are averaged over all wind speed bins weighted according to the wind speed occurrence, to obtain one of the lines in Figure 1. The NWP wind speed is used as reference to determine the wind speed bin for a measurement. For low NWP wind speed the error distribution in wind speed (NWP-truth) gets very skew and the mean true wind speed will be larger than the corresponding NWP wind speed bin average [Stoffelen, 1998]. This explains the large positive residuals. For all but the lowest and highest wind speed bins the pattern as a function of incidence angle is similar. This indicates that the pattern in Figure 1, which is mainly determined by the modal winds is independent of wind speed and thus more likely caused by instrument errors.

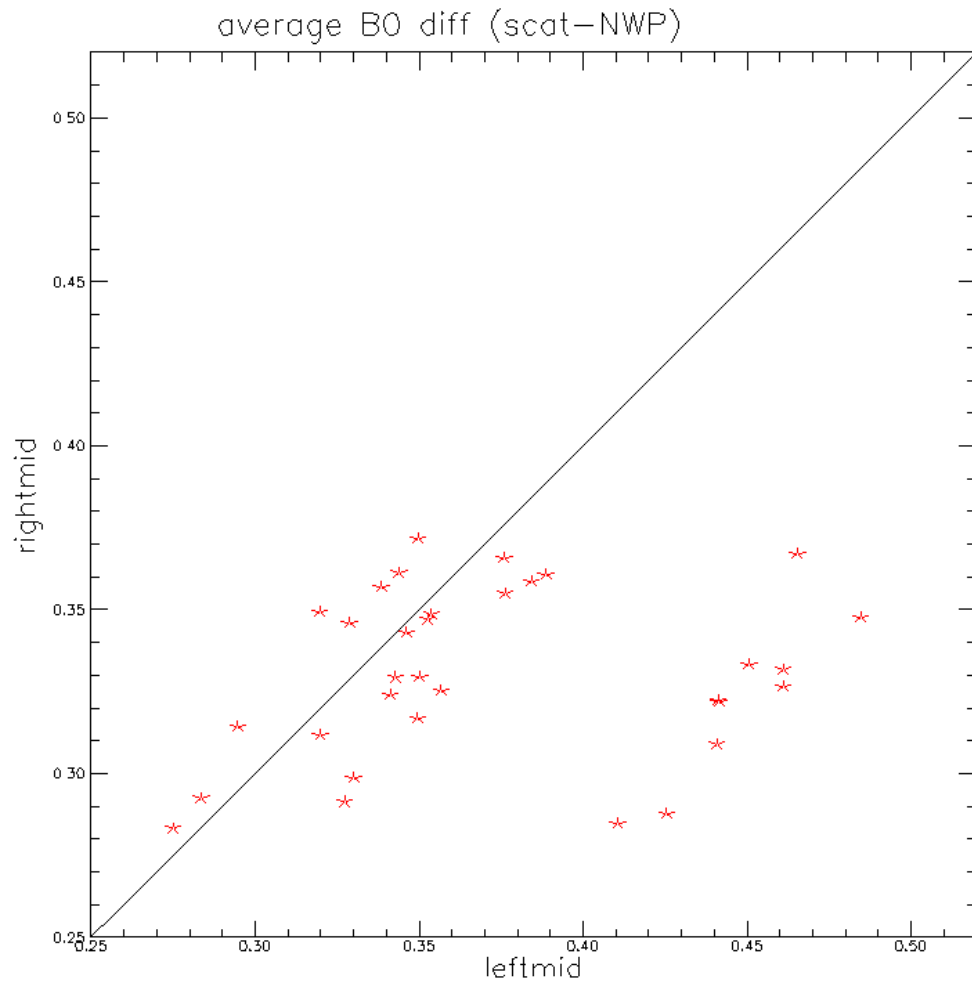


**Figure 2** – Residual of  $B_0$  for the right fore antenna per wind speed bin. NWP ocean calibration is from the period 20090701-20090714 without calval corrections.

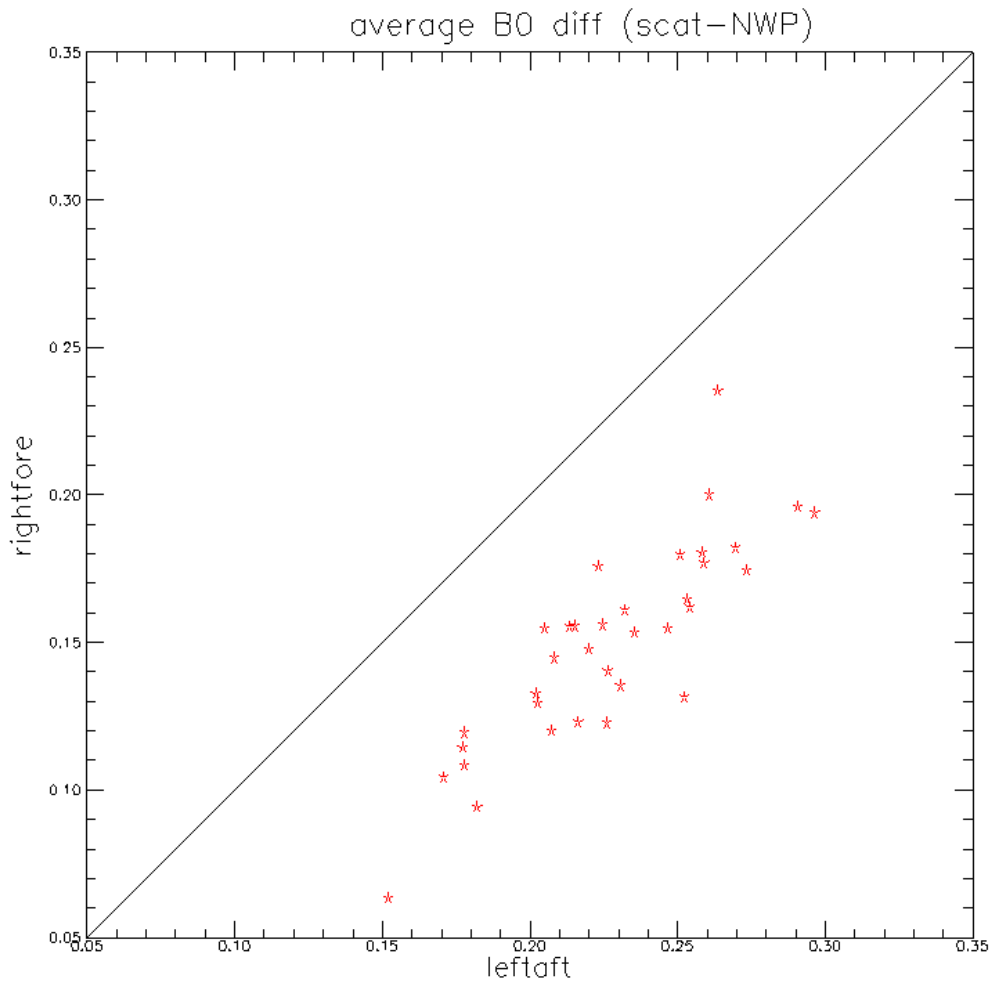
Figure 3 shows a scatter plot of averaged biweekly NOC residuals for opposing pairs of antennas. An opposing pair of antennas, e.g. left fore and right aft, have an opposing orientation with respect to the wind direction distribution. Since the GMF is symmetric over 180 degrees, opposing antennas provide the same NOC error over a given NWP wind distribution and its associated errors. When different parts of the swath have similar wind distribution over a two week period, biweekly NOC residuals for opposing pairs of antennas would become independent of the weather. Thus they are then likely to have a high correlation in NOC residual. Figure 3 shows a high correlation indeed and a scatter of about 0.01 dB, but there is a shift with respect to the symmetry line for the fore and aft antennas such that left fore is 0.060 dB lower than right aft and left aft 0.075 dB higher than right fore. For the mid antenna pair, there are four deviating points with right mid 0.125 dB below left mid, which correspond to the period after the latest level 1B upgrade, from 20090915 to 20091114. These points need further examination and are not used in the NOC correction factor calculation.



a)



b)

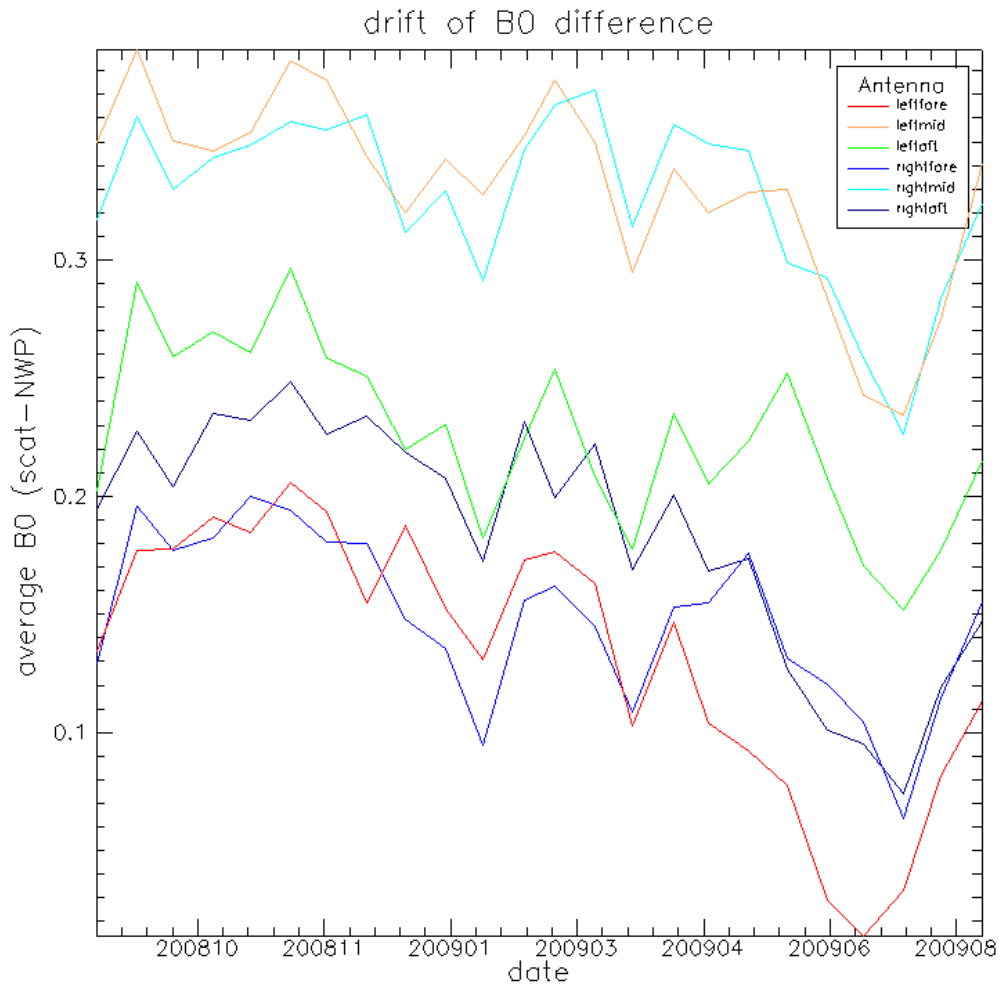


c)

**Figure 3** – Scatter plots of NWP ocean calibration residuals for opposing pairs of antennas. No calval correction is applied. Total period is from 2008-09 to 2010-02.

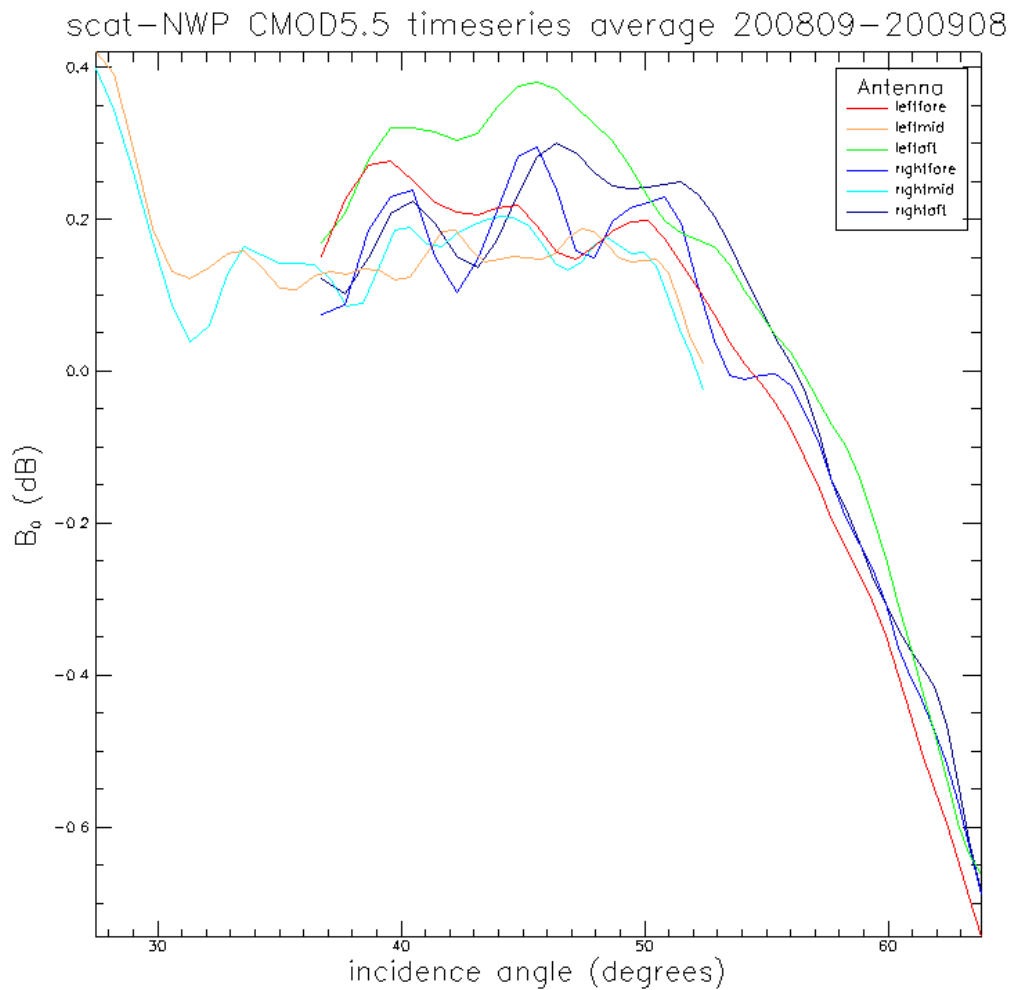
- a) Left fore – right aft
- b) Left mid - right mid
- c) Left aft - right fore

Figure 4 shows a time series for the NWP ocean calibration residual for all antennas. The z difference is averaged over the WVCs in this case. A seasonal variation can be observed corresponding to a seasonal variation in wind speed distribution. The mid antennas are clustering, as well as the fore/aft antennas, indicating some systematic difference in the processing of these fore/aft and mid beams. In our procedure, the input wind direction PDF of the mid beams is different from that of the fore/aft beams mainly due to the trades. Due to errors in the ECMWF wind direction PDF, the filtering to a uniform wind direction is not perfect, possibly resulting in small biases [Stoffelen, 1998]. Due to the seasonal variation in wind PDF it is surprising that the difference in mid and fore/aft beams is so constant over the year. The differences between beams appear rather systematic.



**Figure 4** – Stability over time of the NWP ocean calibration per antenna for ASCAT

Figure 5 shows the average of the NOC residuals over a time series of one year. The time series average will be almost identical to the NOC residuals over one year of data in one run. These values will be tested as NOC cal/val correction factors in AWDP.

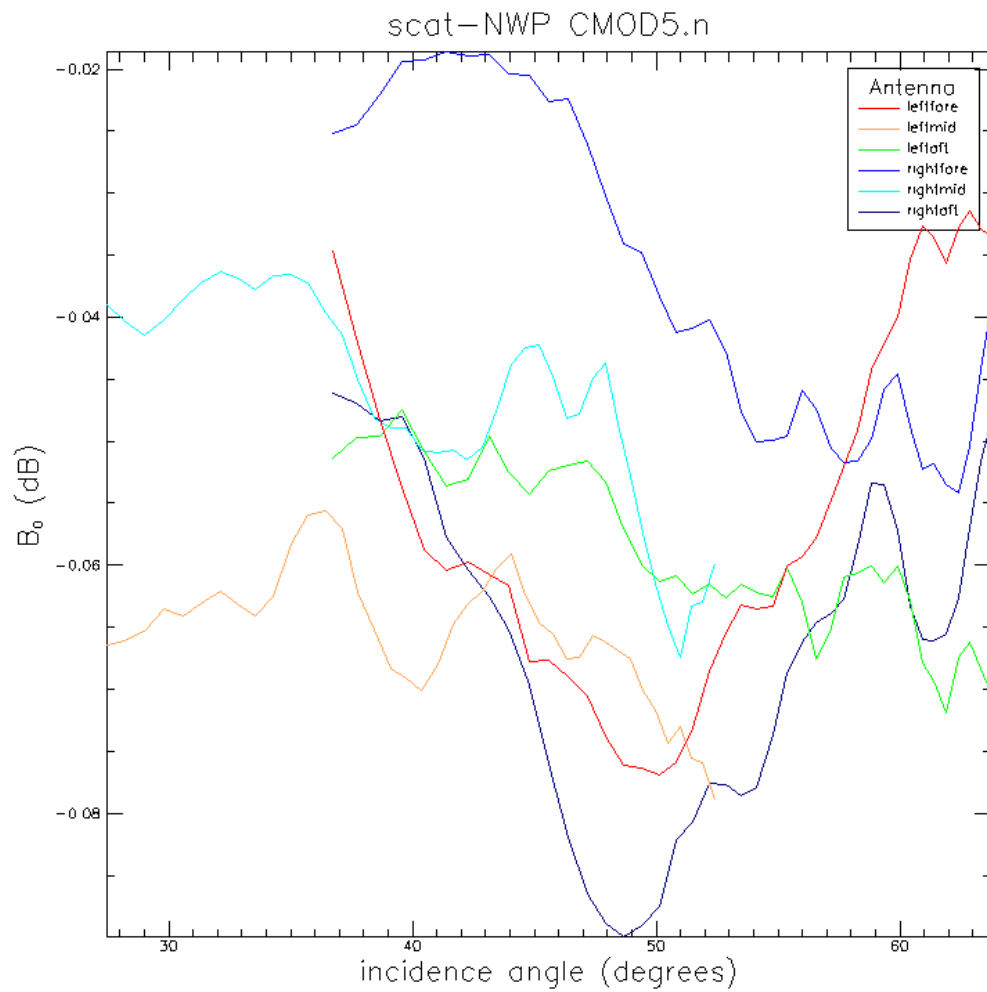


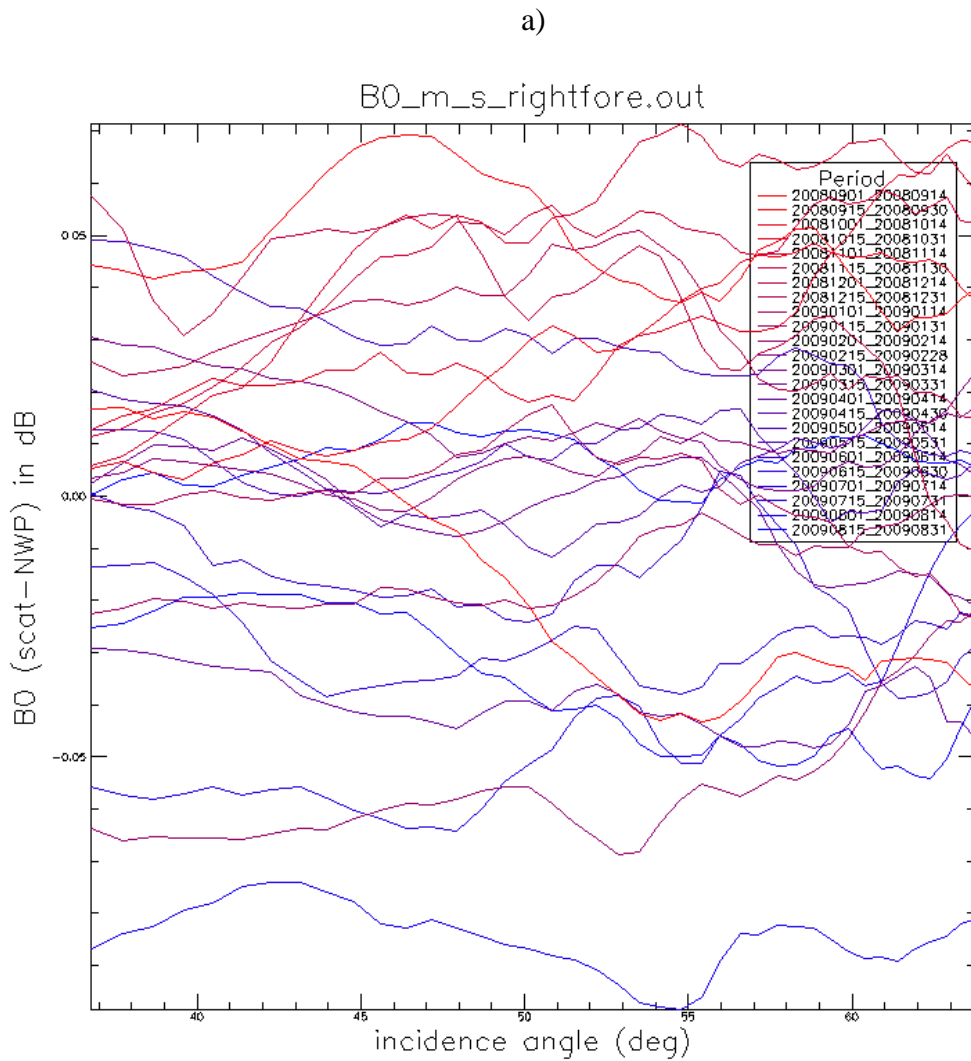
**Figure 5** –Average of the ocean calibration residuals over one year.

## 4 Verification of the NOC correction factors

The residuals from Figure 5 from the one-year period 200809-200908 are stored in a table and may be applied as NOC correction factors in ocean calibration and AWDP.

In order to verify that NOC correction factors have a positive impact on the OC residuals, an OC time series is run over the same one year period from 200809-200908 with the NOC corrections applied. Figure 6a) shows an example of the residuals from an ocean calibration with NOC corrections applied. It shows a spread of typically ~0.1 dB. Figure 6b) shows the residuals during one year of the right-fore beam as a typical example. Also here the spread is small, well below 0.1 dB and shows no systematic patterns.





b)

**Figure 6** – NOC residuals after applying the NOC correction factors.

a) 20090801-20090814

b) Right-fore antenna for all indicated periods in one year

In Figure 7 the time series of the NOC residuals is shown over the one-year period where the NOC corrections from Figure 5 were applied. The vertical offset between beams has been corrected out so that all beam residuals are more close together than in Figure 4 with an average value of zero. All follow similar seasonal trends.

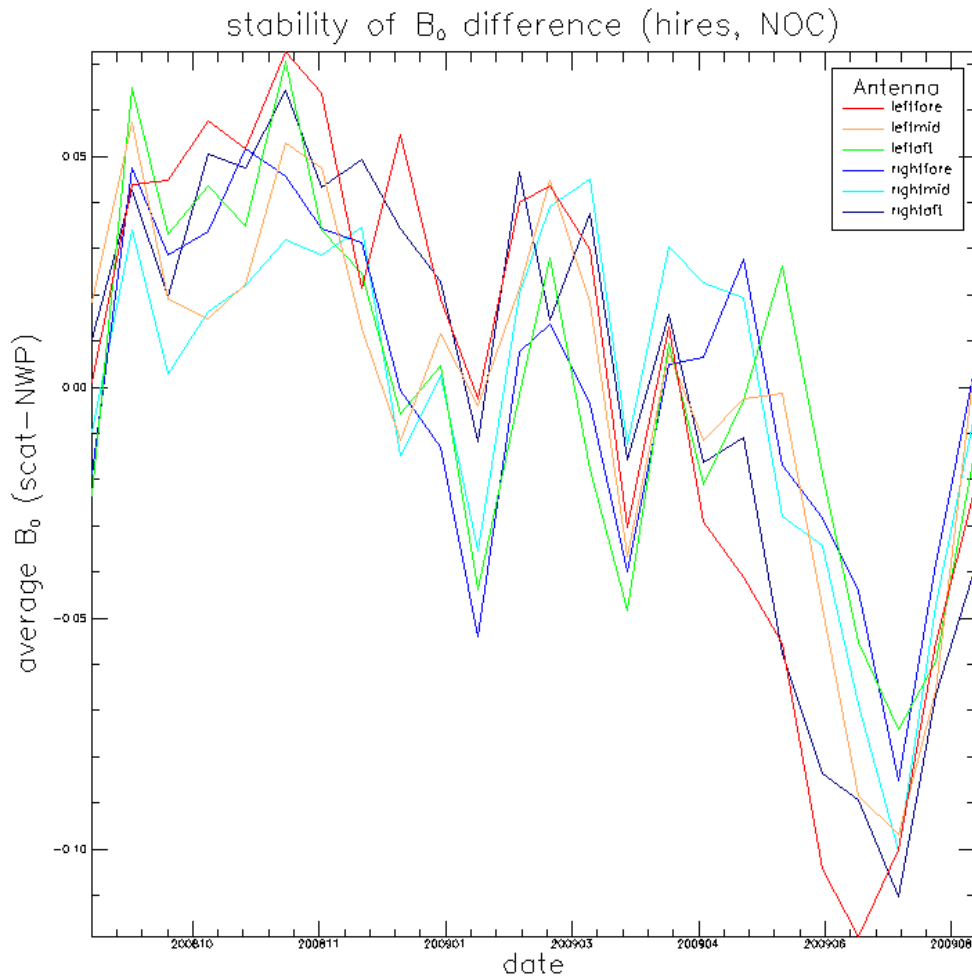


**Figure 7** – Time series over one year of the ASCAT NWP ocean calibration residuals for each antenna. NOC corrections are applied.

## 5 ASCAT stability

The ocean validation can also be used to monitor the stability of the ASCAT. Figure 8 shows a time series over several years using the NOC calibration corrections. A seasonal variation due to global wind distribution changes is clearly visible. The results from all beams are close together showing that interbeam variations are very small.

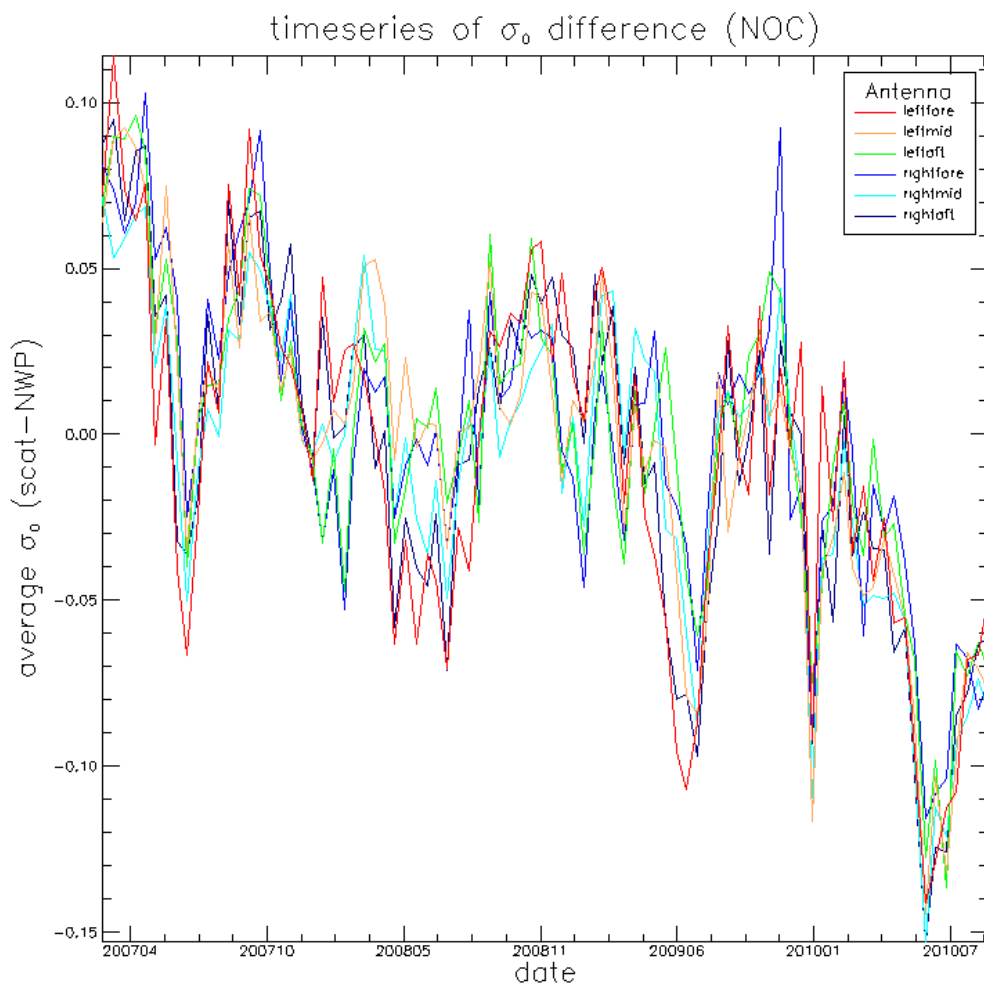
The original results indicated a small step change in the calibration of the left mid beam during September 2009. This change is provisionally corrected in the NOC tables by subtracting 0.125 dB from the left mid beam backscatter value from September 2009 onwards.

A small decrease of the calibration over time can be noticed, which would correspond to a gradual change in the winds. This may be due to changes in the operational ECMWF model over time (the forecasting system is updated twice a year) or a change in ASCAT. To verify such changes, the ASCAT winds are monitored against a set of buoy winds. The

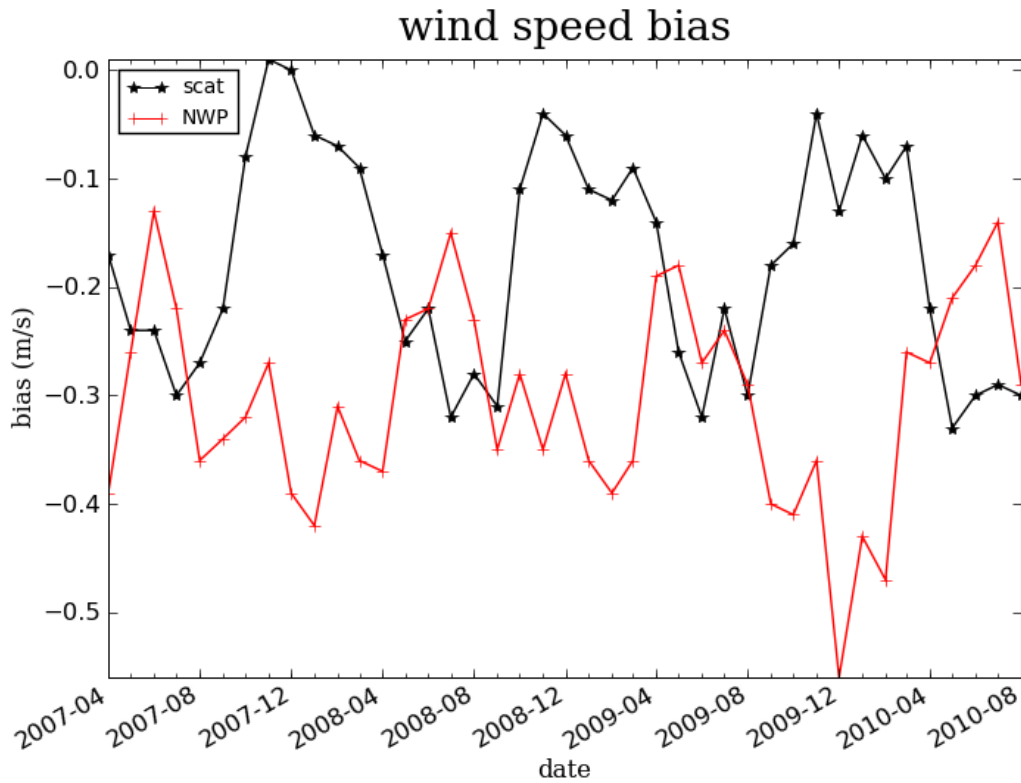
buoys cover the whole globe but are located mainly in the northern hemisphere and tropics (see, e.g. [KNMI site]).

Figure 9 shows the wind speed bias of ASCAT minus buoys and ECMWF minus buoys. Although the spread by seasonal effects on the wind distribution is quite large, the black line (ASCAT-buoys) shows a slightly decreasing trend over time of  $\sim -0.1$  m/s over 3 years that supports the trend in Figure 8, although further evidence is needed to support such subtle change.

A difference of  $\sim 0.1$  m/s in the wind domain corresponds to a difference of  $\sim 0.1$  dB in the backscatter domain on all beams. For the red line (ECMWF-buoys) a trend is not clearly detectable. In November 2008 the transition from cmod5.5 to cmod5.n (equivalent neutral winds) is made in the operational processor. This has an effect on the ASCAT winds which is compensated for in the figure. Some other minor changes in the operational processor (QC) remain.



**Figure 8** – Time series of ASCAT NWP ocean calibration residuals for each antenna. NOC corrections are applied. All level 1b backscatter changes are compensated by reverse corrections.



**Figure 9** – Time series of ASCAT and NWP buoy wind biases from a triple collocation data set. All level 1b backscatter changes are compensated by reverse corrections.

To illustrate the aforementioned seasonal variation in NWP wind in Figure 10 the zonal and meridional ECMWF wind components  $u$  and  $v$  are shown over several years. Each point in the figure corresponds to an averaged value of the ocean wind component over a period of two weeks. Clearly a seasonal variation especially in the meridional component can be seen. A study with simulated NWP data has shown that variations in NWP wind distribution have an influence on the ocean calibration residuals.

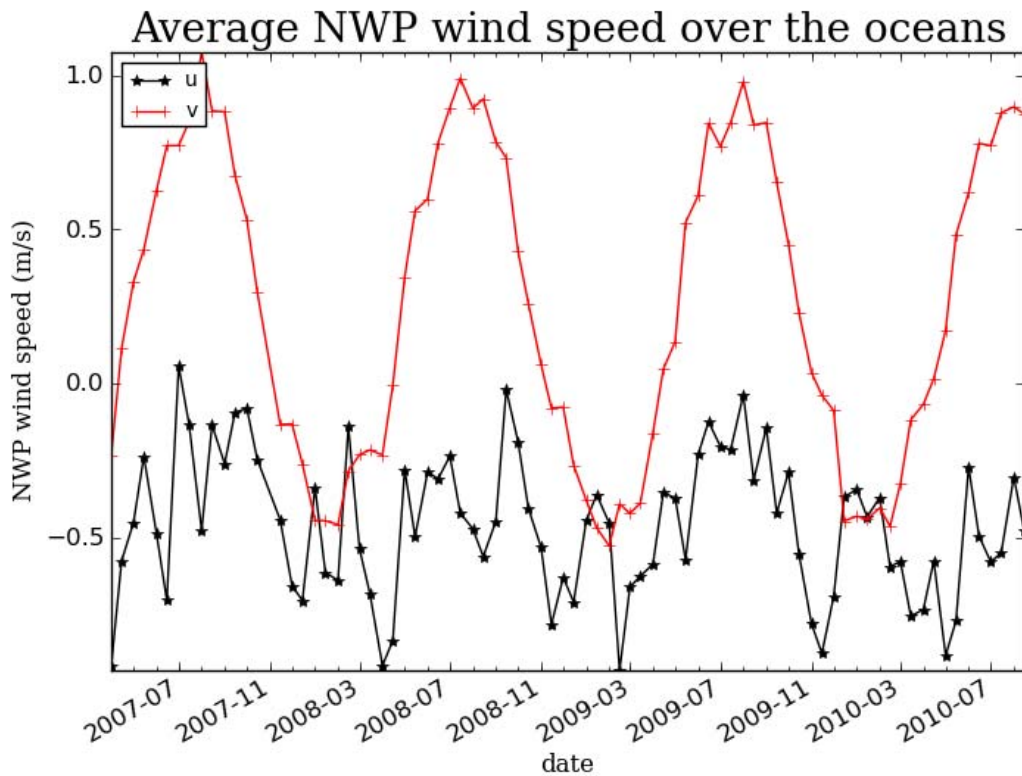


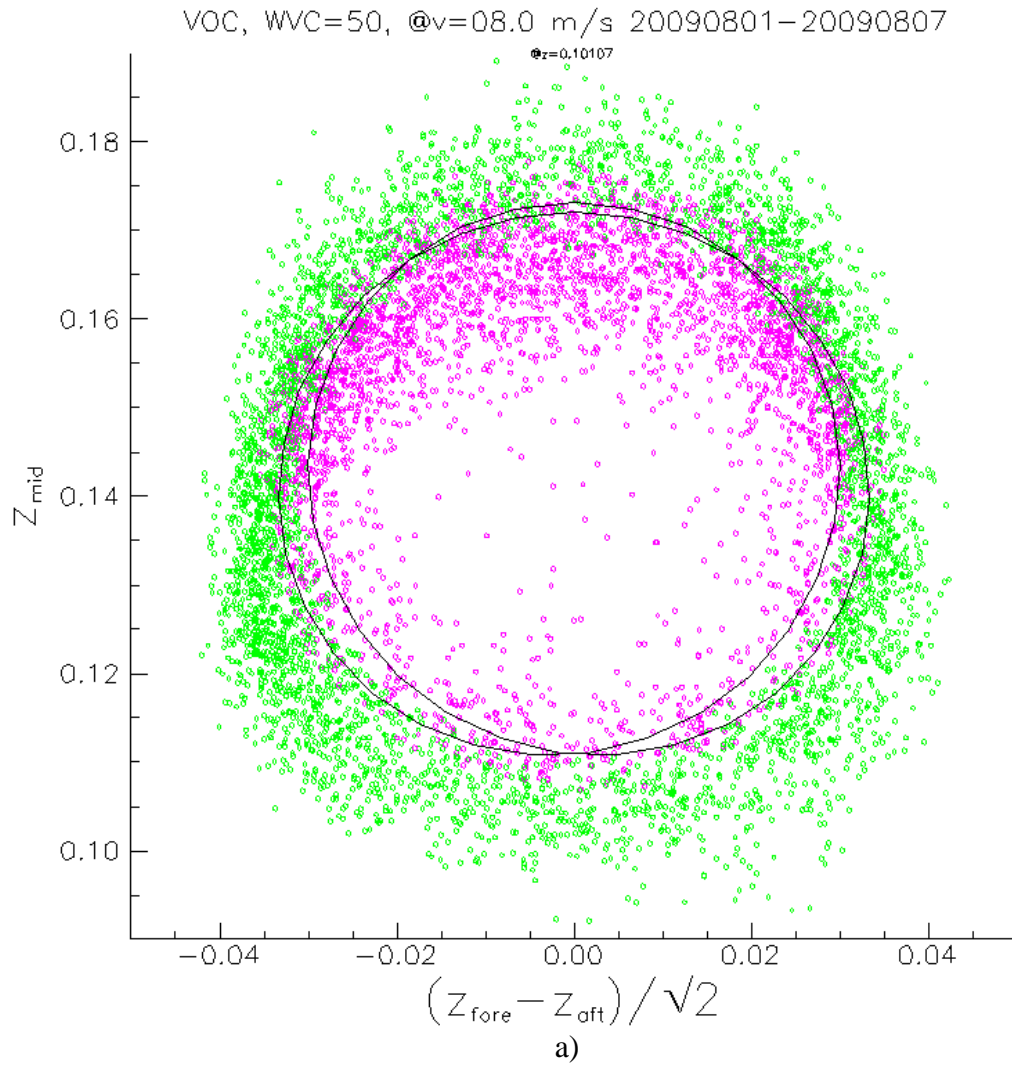
**Figure 10** – Time series of NWP zonal and meridional wind components  $u$  and  $v$ . Each point corresponds to an averaging over two weeks NWP data over the oceans.

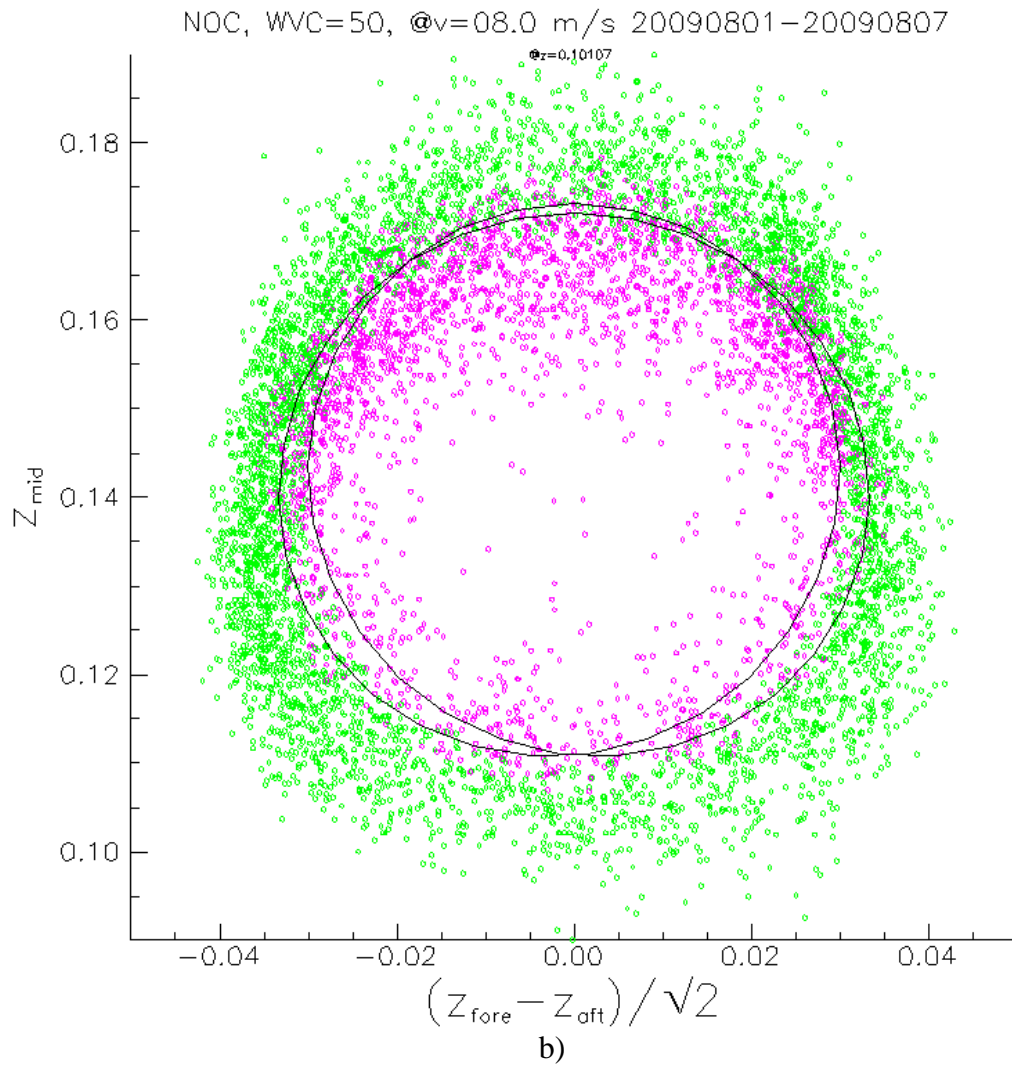
## 6 Visualisation

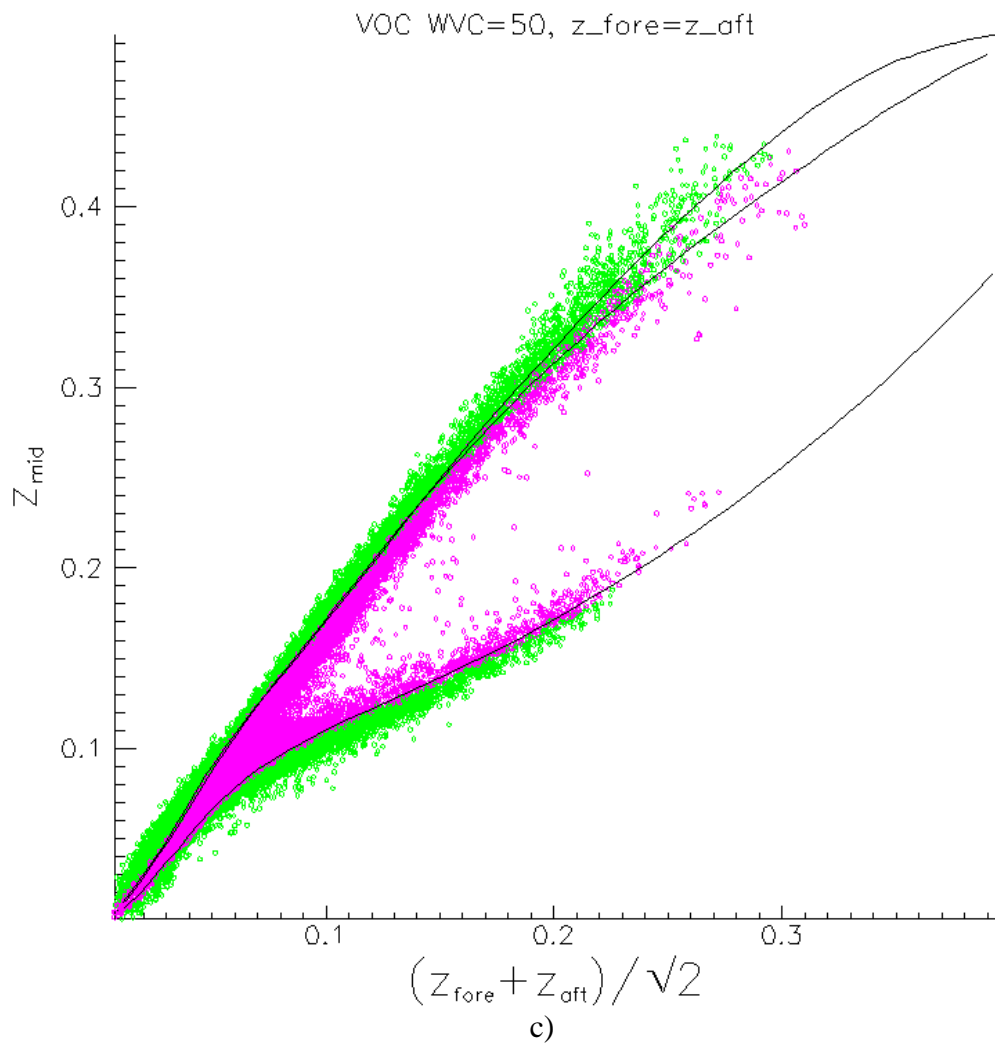
Visualisations of the data triplets in measurement space together with the GMF have been made in order to see how well the GMF fits the cloud of measurements. Purple triplets have a positive MLE and lie inside the cone, green triplets have a negative MLE and lie outside the cone. WVC 26 is chosen which is on the right swath, has incidence angles fore/aft=43.95°, mid=33.64°, and roughly corresponds to the middle swath WVC 10 of METOP’s predecessor the European Remote sensing Satellite (ERS). CMOD5 was developed for ERS and is well established for these incidence angles. (CMOD5.n has the same shape as CMOD5 in visualisation space, only the wind speed parameterisation is different).

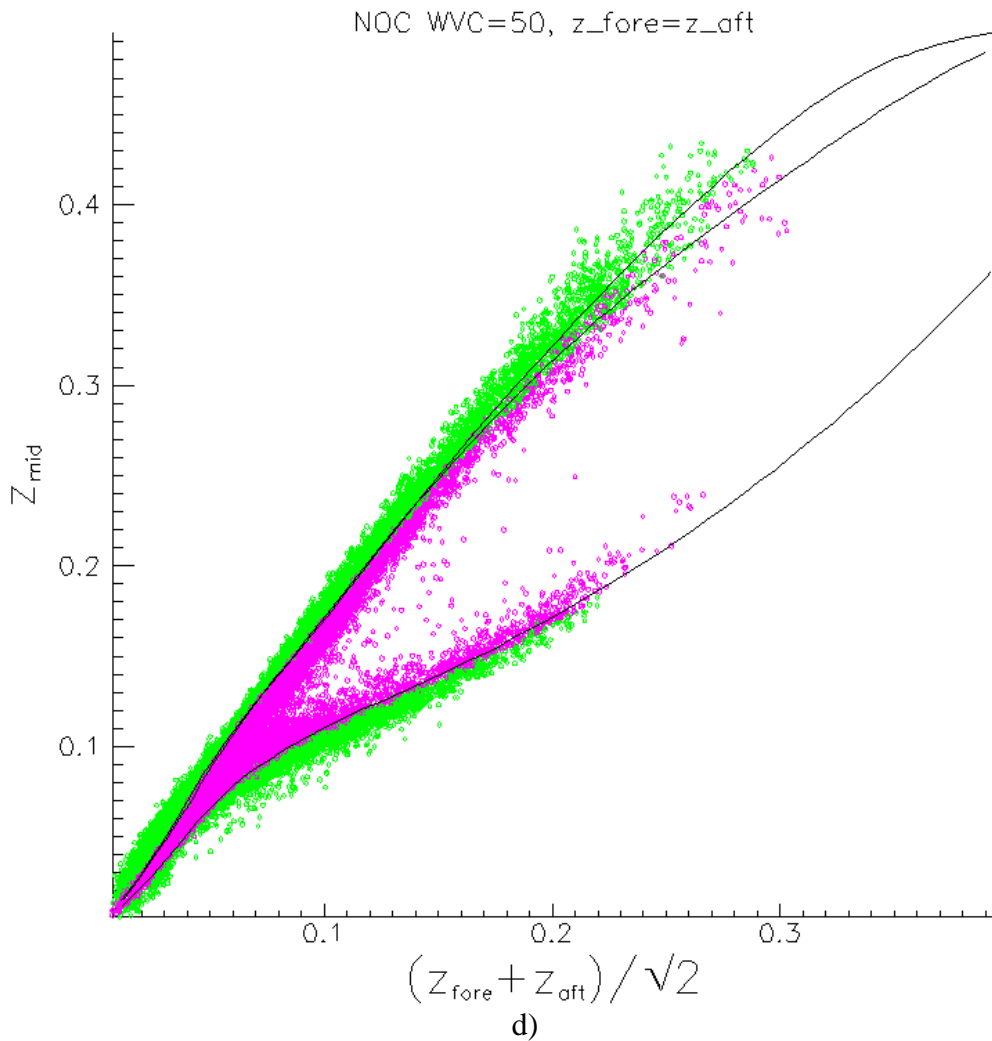
Figure 11a) and Figure 11b) show the cone cross section at the modal wind speed  $V=8$  m/s for VOC and NOC respectively. Both figures show a good fit. Purple triplets have a positive MLE and lie inside the cone, green triplets have a negative MLE and lie outside the cone. Note that the colours are mixed in the vicinity of the GMF cross section due to the fact that triplets within a slice of a certain depth are plot and the GMF is only shown for the middle of this slice. In the NOC case the purple/green symmetry is somewhat better, indicating a slightly better fit.

Figure 11c) and Figure 11d) show the  $z_{\text{fore}}=z_{\text{aft}}$  intersection with the cone. Also here the figures show a good fit. Similar results are obtained for other WVCs in both the left and right swath, with in general a slightly better symmetry for the NOC case.









**Figure 11** - Visualisation of CMOD5.n for WVC 50 (right swath, incidence angle fore/aft=43.97°, mid=33.57°) together with data triplets (correction is applied on the data triplets). Purple triplets have a positive MLE and lie inside the cone, green triplets have a negative MLE and lie outside the cone. One week of data is used from 20090801 to 20090807.

- a) Intersection of the cone with the plane  $(z_{fore} + z_{aft}) / \sqrt{2} = z_{ref}$  for WVC number 50. The value of  $z_{ref}$  is 0.10107, the  $z_{mid}$  value at wind direction  $\phi=0$  and corresponding to a wind speed of 8.0 m/s. Triplets within a distance of  $\pm 0.02 z_{ref}$  from the mentioned plane are plotted. VOC corrections are applied.
- b) as a) with NOC corrections applied.
- c) Intersection of the cone with the plane  $z_{fore} = z_{aft}$  for WVC number 50. Triplets within a distance of  $\pm 1.0$  dB from the mentioned plane are plotted. VOC corrections are applied.
- d) as c) with NOC corrections applied.

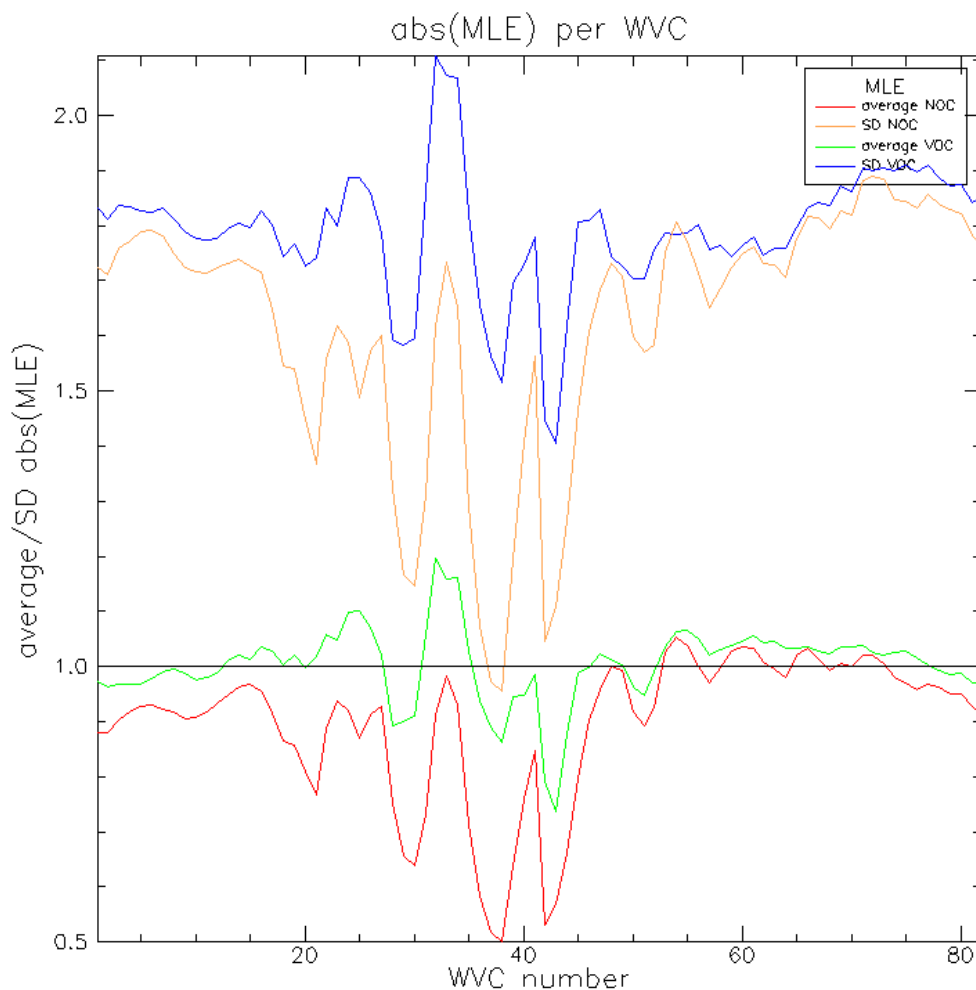
## 7 MLE normalisation and QC

The Maximum Likelihood Estimate (MLE) is the distance from a measurement triplet to the point on the wind cone in 3D measurement space that corresponds to the retrieved

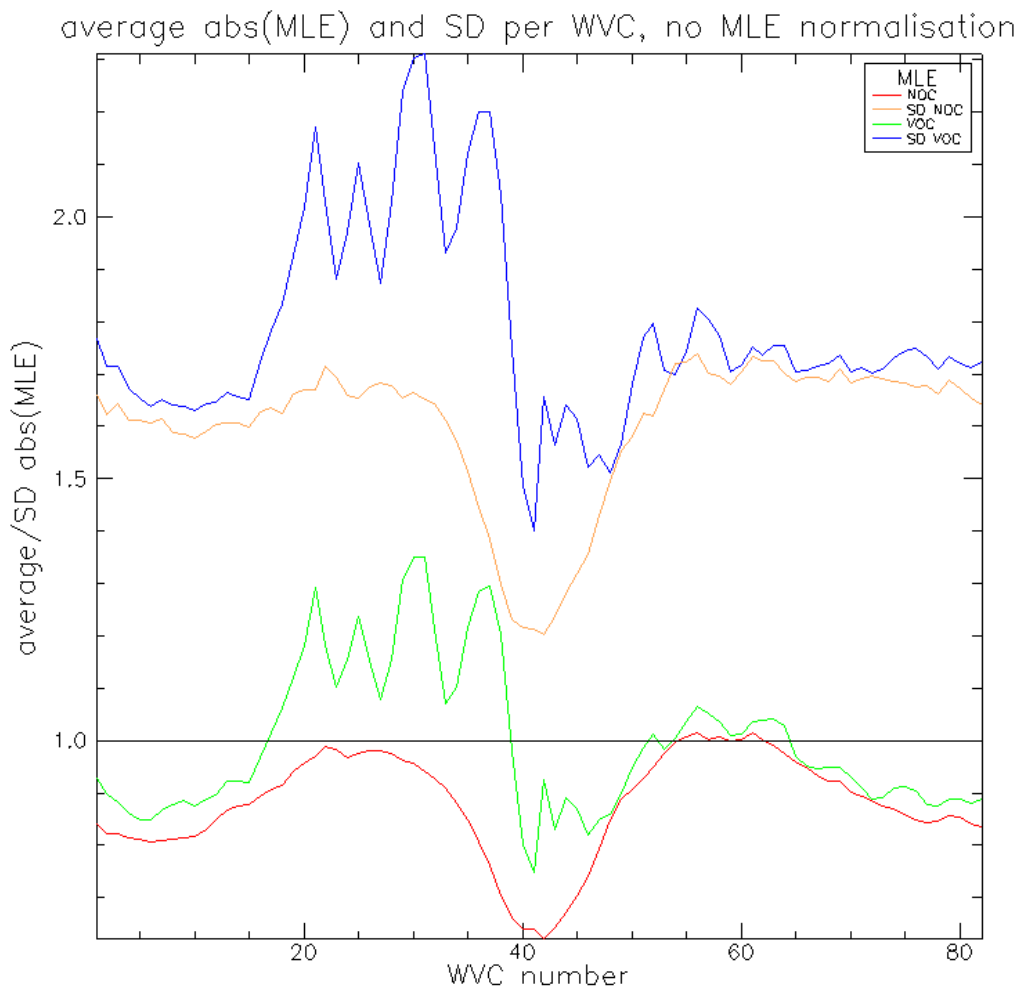
wind. It is a measure of how well the measurements and GMF fit to each other. The MLE is normalised using a table in order to get an expectation value of  $\langle \text{MLE} \rangle = 1$  for each WVC.

Figure 12a) shows the absolute MLE value per WVC for the NOC and VOC correction case. The values of the absolute MLE are averaged over one week of data. The NOC case in Figure 12a) shows slightly lower values, especially for the left swath. Also it seems to be more asymmetric and less smooth than the VOC case. This is largely caused by the WVC dependent MLE normalisation factors. These factors are used to make the average MLE value WVC independent and to give them an expectation value of  $\langle \text{MLE} \rangle = 1$ . They were derived for the VOC case and do a good job in smoothing the MLE values and making them symmetrical in the VOC case.

In the NOC corrected case any WVC dependency caused by small interbeam biases is already corrected out by the NOC corrections itself, and without the normalisation factors the MLE would be a smooth function of incidence angle. This is shown in Figure 12b) where data is used that is reprocessed with the NOC/VOC corrections but without MLE normalisation factors. Here indeed the MLE is a smooth and symmetrical function for the NOC case, but shows irregularities for the VOC case.



a)



b)

**Figure 12** – Average/SD of the absolute value of the MLE per WVC for one week of data  
 a) NOC and VOC case, MLE normalisation factors and QC thresholds derived from VOC data are applied.  
 b) NOC and VOC case, no MLE normalisation factors are applied, QC threshold derived from VOC data are applied.

AWDP uses MLE normalisation tables to ease QC and monitoring on the basis of the MLE. Without normalisation the MLE distribution shows variations as a function of WVC that are related to GMF errors and the exact 3D shape of the GMF cone in 3D measurement space. Backscatter calibration causes (small) changes to the cone location in measurement space and thus requires new normalisation tables. The average and SD of the absolute value of the MLE as a function of WVC number (see Figure 12b) are input for an iterative process to calculate new MLE normalisation and QC threshold tables using only winds > 4 m/s. (see Annex). These tables are stored to a file and read in by AWDP. Figure 13 shows the values for the MLE normalisation and QC threshold used in combination with the VOC and NOC correction factors.

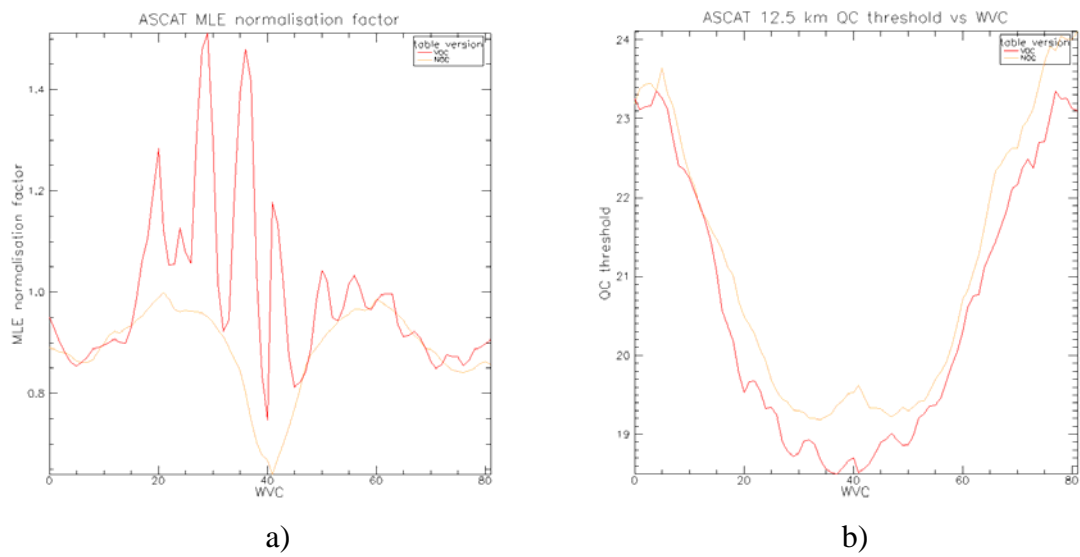


**Figure 13** – a) MLE normalization factors and b) QC threshold settings per WVC used in the wind processor AWDP. Shown are the values used in combination with the VOC correction factors and the new values used in combination with the NOC correction factors.

The new normalization and QC have a small effect on data selection and product validation, which we tested. One week of ASCAT data is reprocessed with the NOC correction table and the new MLE normalization and QC thresholds. The MLE statistics for the NOC corrections with the new tables (see Figure 14) show a more symmetric behaviour as compared to Figure 12a) where the original tables were used.

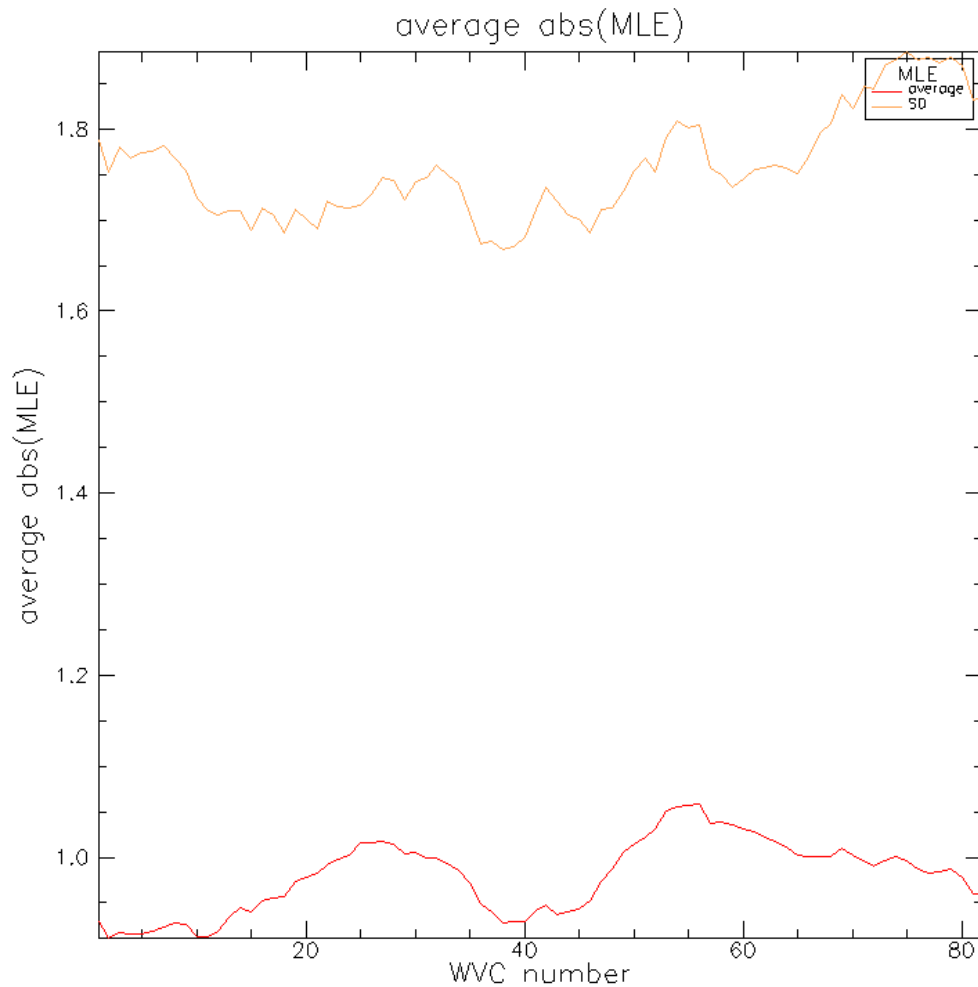


**Figure 14** – MLE average and SD as as function of WVC number from one week of ASCAT data. The NOC correction table is used as well as the new MLE normalisation and QC thresholds.

## 8 Effects of NOC and new QC tables

One week of ASCAT data (20090801-20090807) is reprocessed using AWDP with the NOC corrections applied together with the new MLE normalisation and QC threshold tables, in order to compare the resulting statistics with the operational values where VOC corrections were applied. In sections 8.1, 8.2 and 8.3 the effect of the NOC corrections on respectively wind statistics, QC and MLE statistics is examined.

### 8.1 Wind statistics

The wind speed bias (scatterometer wind speed minus NWP wind speed) as a function of WVC is calculated for the reprocessed data with NOC correction and the operational data with VOC correction in Figure 15). The NOC case shows a symmetric pattern for the left and right swath, whereas for the VOC case the bias shows less symmetry. A symmetric pattern is expected from a physical point of view and implies that the bias may be

described as a function of incidence angle instead of as a function of WVC. The standard deviation (SD) is comparable in both cases as well as the average value of the bias. The NWP 10-m winds were transformed into equivalent neutral winds. The resulting biases are slightly positive on average.

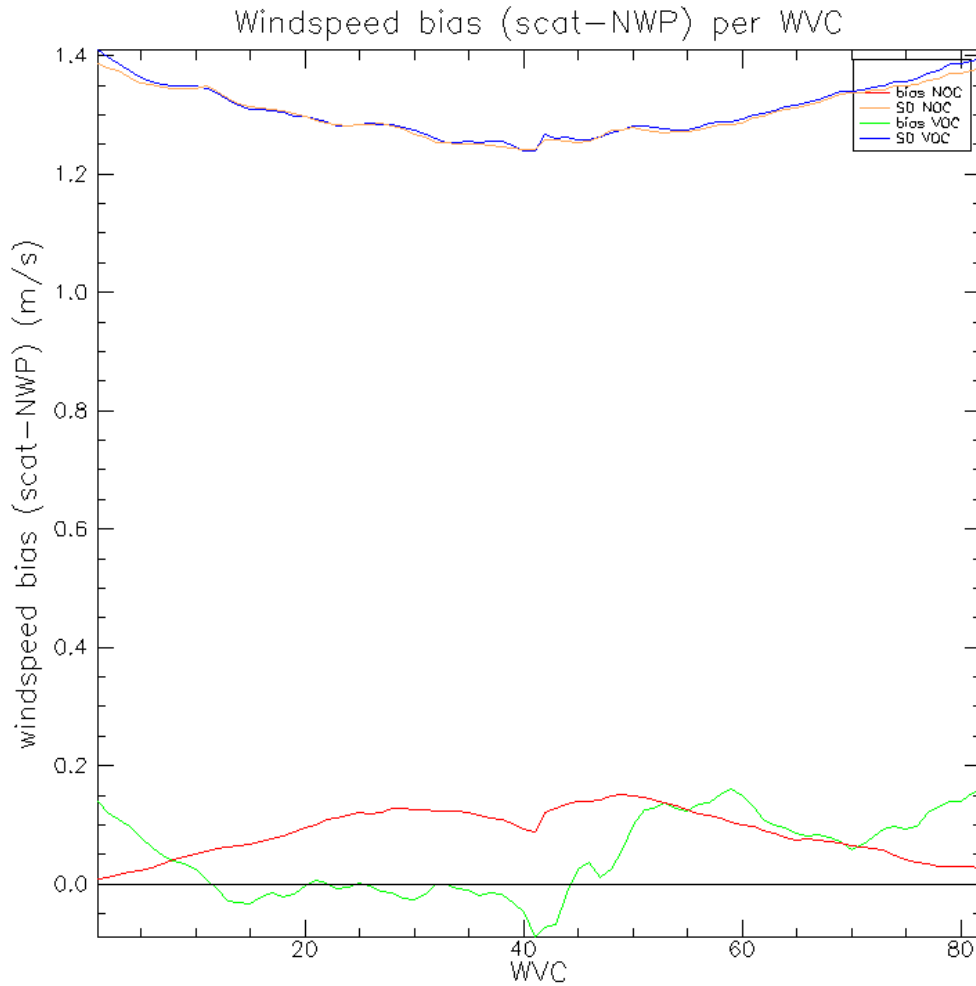


**Figure 15** – Wind speed bias and SD per WVC for one week of data, for NOC and VOC

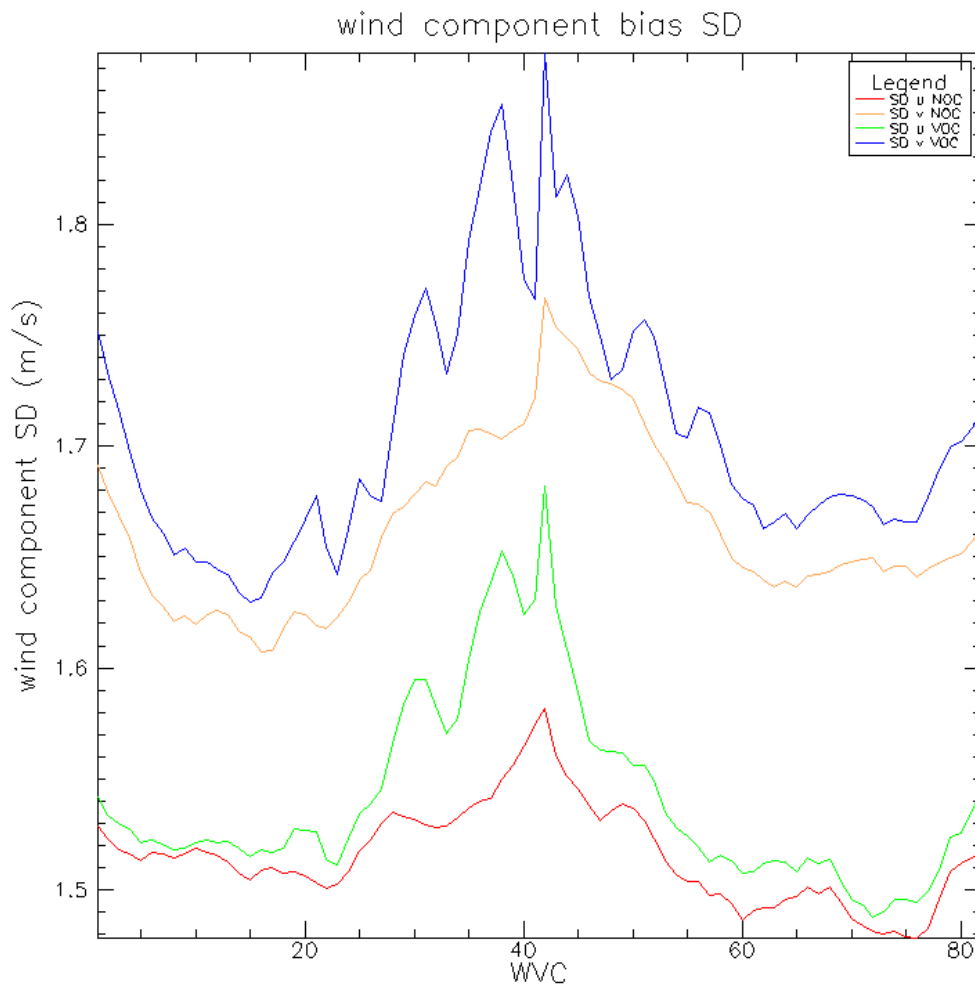


**Figure 16** – u and v wind component SD of difference ASCAT minus ECMWF as a function of WVC, NOC and VOC case.

Figure 16 shows the u and v wind component SD of difference ASCAT minus ECMWF as a function of WVC. The patterns are comparable for the NOC and the VOC correction case, but are systematically lower for the NOC case, denoting an improved wind retrieval for NOC. Table 1 summarises the wind statistics in terms of bias and standard deviation for the two cases. The NOC correction case has better statistics than the operational case (VOC). SD values for wind speed V, wind direction phi and wind components u and v are all slightly lower.

**Table 1** – Wind statistics for NOC correction and VOC correction

	Bias NOC	Bias VOC	SD NOC	SD VOC
V	0.09 m/s	0.05 m/s	1.30 m/s	1.31 m/s
$\phi$	-0.06°	0.29°	15.79°	16.36°
u	-0.17 m/s	-0.16 m/s	1.52 m/s	1.54 m/s
v	-0.05 m/s	-0.03 m/s	1.66 m/s	1.71 m/s

## 8.2 Quality flags

The occurrence ratio of some important level 2 quality flags and their WVC dependency is shown in Figure 17 for the NOC and VOC case. In both cases the applicable MLE normalisation and QC threshold tables are used. The differences between these two cases are again favourable for NOC with a smoother curve for the KNMI QC flag and GMF\_distance flag and less points rejected by the 2DVAR spatial inconsistency flag (var\_qc). The GMF\_distance flag is set when the measured triplet has an anomalously large distance to the GMF cone, while the var\_qc flag is set during 2DVAR ambiguity removal when a wind vector is spatially inconsistent with its neighbours.

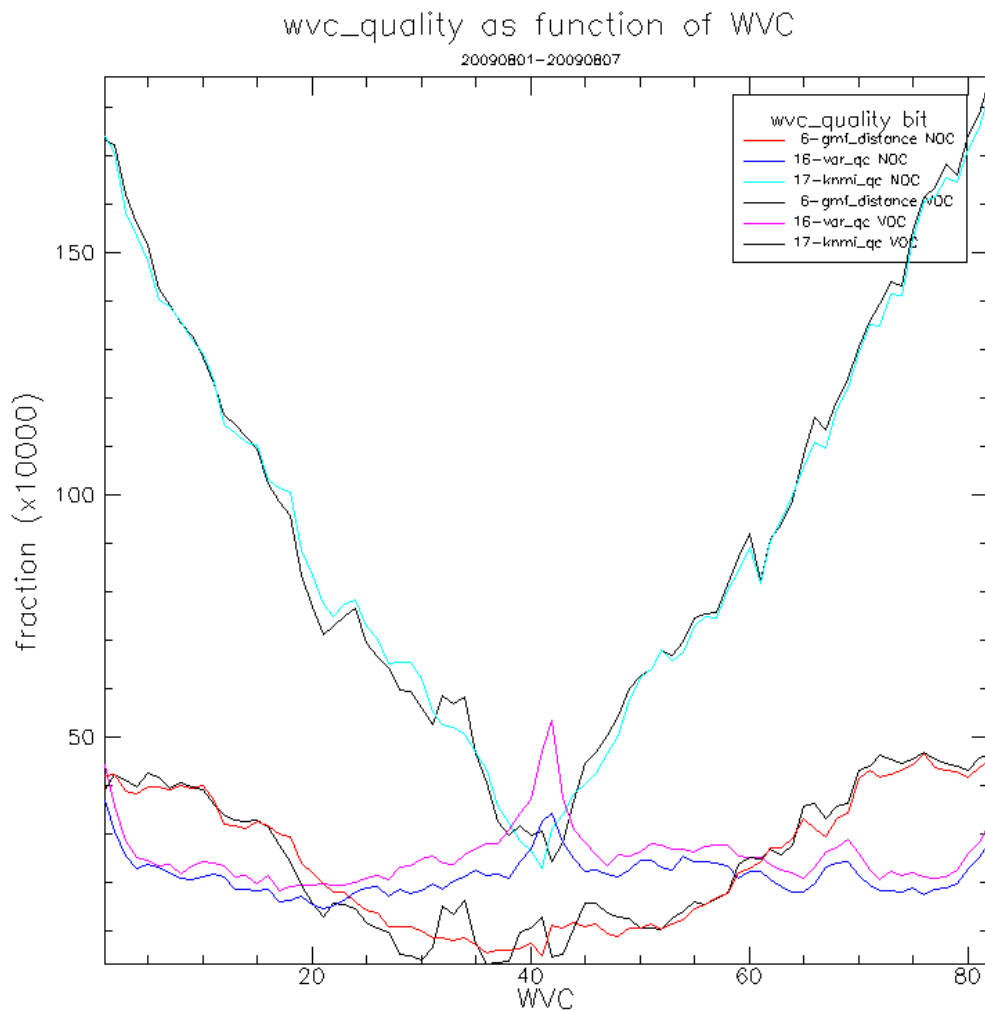
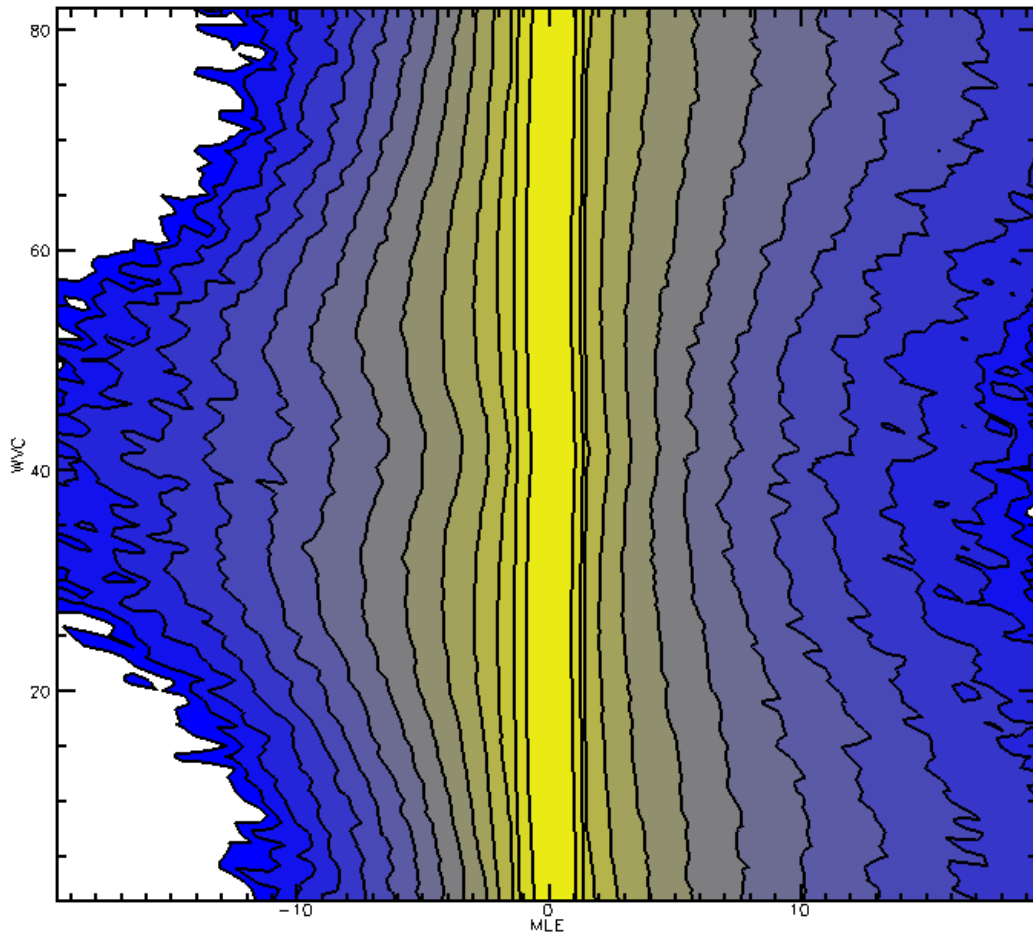


**Figure 17** – Some level 2 quality flags as a function of WVC from one week of data

## 8.3 MLE distribution

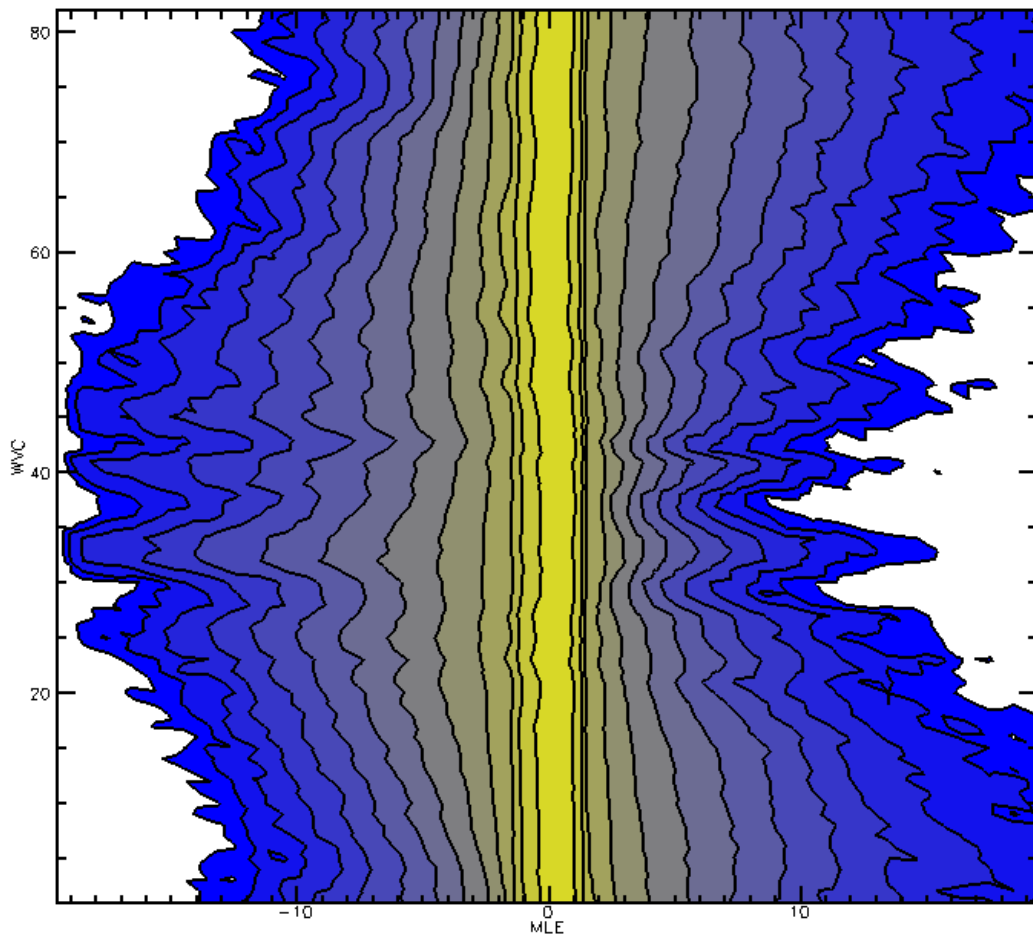
Figure 18 shows the MLE distribution as a function of WVC. Figure 18a) shows the NOC case where the new MLE normalisation and QC threshold tables are used. It shows a clear symmetry for the left and right swath. The VOC case in Figure 18b) on the other hand lacks symmetry and shows irregularities, indicating poorer calibration.

MLE vs WVC (NOC with new MLE table)



a)

MLE vs WVC (VOC)



b)

**Figure 18** – MLE distribution as a function of WVC number from one week of ASCAT data.  
 a) The NOC correction table is used as well as the new MLE normalisation and QC thresholds.  
 b) The VOC correction table is used as well as the corresponding MLE normalisation and QC thresholds.  
 The MLE distribution colours change at each solid line which is drawn at every factor of 2 increase or decrease in the distribution.

## 9 Conclusions

On many points the NOC gives results that are comparable with, or better than the VOC method:

- The two-weekly NOC residuals for data with the year-average NOC corrections applied are small, within  $\sim 0.1$  dB from each other over the full observed one year period. This shows the consistency in the approach;

- The AWDP wind speed bias against ECMWF is small, but becoming symmetric for the left and right swath when the NOC corrections are applied;
- The AWDP-ECMWF wind speed, direction and component SDs are reduced for NOC with respect to the VOC-correction processed winds;
- The MLE is reduced by up to 40% in certain WVCs when NOC corrections are used with respect to the MLEs produced by AWDP with VOC corrections. Moreover, following expectations the MLE is becoming symmetric for the left and right swath when the MLE normalization factors are omitted.
- The reduction in level 2 QC flag occurrences for NOC-corrected AWDP compared to the VOC case is about 10% for the MLE check and the 2D-VAR spatial consistency check.

The NOC correction factors are averages over a one-year period. The NOC correction factors are dependent on incidence angle (WVC) and beam. They will compensate for any error, irrespective of the source of the error, whether it is an error in the GMF, in the radiometric calibration of the scatterometer, or interbeam biases. On the other hand the VOC method makes use of a visual correction, judged by eye, and a multiplication factor to correct for the wind speed to implement a WVC and beam dependent correction. The VOC method was not focused on the modal winds and too much tuned towards the more extreme winds occurring at the different WVCs. The NOC-corrected backscatter triplets thus visually better fit the GMF cone at the modal wind speeds.

Implementation of the NOC corrections together with new MLE normalization factors is useful and leads to slightly better wind, QC and MLE statistics where the asymmetry between left and right swath is diminished. The MLE normalisation results in appropriate QC thresholds and monitoring flag settings for the NOC implementation.

The NOC residuals for high resolution mode reveal more detail than the residuals for nominal resolution. The NOC corrections for the high resolution mode (12.5 km) and nominal resolution mode (25 km) are calculated and used separately. Using nominal mode corrections that are derived from the high resolution mode corrections would lead to insufficient accuracy at the swath edges.

Reprocessing the ASCAT data using the NOC corrections, as well as the newly derived MLE normalization and QC threshold tables, yields good-quality wind and MLE statistics, slightly better than with the VOC method. Moreover, the distributions are more symmetric for left and right swath and show a dependence on incidence angle only.

In a later stage the symmetrical and beam-independent part of the correction can be put in a new version of the GMF. It should subsequently be tested whether the remaining small beam-dependent correction part affects the wind retrieval process.

The NOC corrected backscatter data form a good basis for further GMF improvements using MLE residual analyses as a function of incidence angle, wind speed and wind direction.

# Annex – Tuning of AWDP MLE normalisation and Quality Control threshold tables

## General considerations

- This work has been done in June and July 2008.
- This work has been done using ASCAT 25-km data from 21 Dec. 2007 to 20 Jan. 2008 (both inclusive) and ERS data from 1 Jan. 1993 to 31 Jan. 1993 (both inclusive). It has been repeated with ASCAT 25-km and 12.5-km data from 20 Sep to 19 Oct 2008 (both inclusive) to calculate the final tables that were checked in in CVS.
- In the wind inversion, the CMOD5.n GMF for neutral winds was used.
- The following awdp command line options were used: -noamb -nowrite -ignore12flags -cmod 5n -calval -handleall
- All WVCs with lat > 55 or lat < -55 degrees were skipped to exclude any ice contamination (temporary code change in awdp\_inversion.F90, subroutine invert\_node).

```
! set qual_sigma0 flag outside -55 - +55 degrees lat and return
if (c11%lat .gt. 55.0) then
  c11%wvc_quality%qual_sigma0 = .true.
  return
endif
if (c11%lat .lt. -55.0) then
  c11%wvc_quality%qual_sigma0 = .true.
  return
endif
```

- The geophysical noises were calculated using the tables obtained from MarcosPortabella on 7 Mar. 2008 (ascat\_25000\_geoph\_kp\_vs\_speed\_and\_inc\_ang.asc) and on 27 Feb. 2007 (ers\_25000\_geoph\_kp\_vs\_speed\_and\_inc\_ang.asc). NOTE: for ASCAT 12.5, the geophysical noise is assumed to be half the value from the 25-km table.
- Only those wind solutions closest to the ECMWF forecast winds in the BUFR data have been considered.

## Step 1

- Use a MLE normalisation table (ascat\_25000\_MLE\_norm\_vs\_wvc.asc or ers\_25000\_MLE\_norm\_vs\_wvc.asc) containing values of 1.0 for all WVC numbers.
- Consider only wind solutions with wind speed of > 4 m/s.
- Process all data and write for each wind solution the node number and the absolute value of the conedistance, see code below to be inserted in post\_inversion.F90, subroutine normalise\_conedist\_ers\_ascat.

## ASCAT NWP Ocean Calibration

```
v = inv_output%foundwindspeed(closest)
...

! normalise the cone distances for each solution
do isol = 1,inv_output%nr_of_windsolutions
  inv_output%conedistance_measured(isol) = inv_output%conedistance_measured(isol) / &
    (kp_total_norm * node_dependent_norm_factor)
enddo

! temporary code
if (v .gt. 4.0) then
  write(34,'(I2.2,F8.3)') inv_input%node_nr, &
    abs(inv_output%conedistance_measured(closest))
endif
! temporary code
```

- From the resulting output file fort.34, calculate the mean absolute cone distance vs. node number, using the small Fortran program calc\_mean\_mles.f.
- This yields new MLE normalisation tables:  
ascat\_25000\_MLE\_norm\_vs\_wvc.asc\_step1 and  
ers\_25000\_MLE\_norm\_vs\_wvc.asc\_step1.

## Step 2

- Repeat step 1, but with some changes.
- Use the MLE normalisation tables obtained in step 1 in the next processing.
- Use only wind solutions with with wind speed of  $> 4$  m/s and absolute MLE of  $\leq 18.45$ .
- Process all data and write for each wind solution the node number and the absolute value of the conedistance.

```
v = inv_output%foundwindspeed(closest)
...

! normalise the cone distances for each solution
do isol = 1,inv_output%nr_of_windsolutions
  inv_output%conedistance_measured(isol) = inv_output%conedistance_measured(isol) / &
    (kp_total_norm * node_dependent_norm_factor)
enddo

! temporary code
if (v .gt. 4.0) then
  if (abs(inv_output%conedistance_measured(closest)) .gt. 18.45) then
    write(35,'(I1)') 1
  else
    write(35,'(I1)') 0
    write(34,'(I2.2,F8.3)') inv_input%node_nr, &
      abs(inv_output%conedistance_measured(closest))
  endif
endif
! temporary code
```

- From the ratio between the number of '1' occurrences and the total number of occurrences in fort.35, the rejection rate can be computed. It appears to be approximately 0.47% for ASCAT 25-km and 0.44% for ERS. For ASCAT 12.5-km we get approximately 0.28% rejections in Sep/Oct 2008.

## ASCAT NWP Ocean Calibration

- From the resulting output file fort.34, calculate again the mean absolute cone distance vs. node number.
- This yields new MLE normalisation tables:  
ascat\_25000\_MLE\_norm\_vs\_wvc.asc\_step2 and  
ers\_25000\_MLE\_norm\_vs\_wvc.asc\_step2.

### Step 3

- Calculate the final MLE normalisation tables through multiplying the tables from step 1 and step 2 WVC-by-WVC.
- Calculate the QC threshold tables for each WVC number as  $18.45 / ((\text{MLE norm from step 2}) * 9.0) = 2.05 / (\text{MLE norm from step 2})$ . This is also done WVC-by-WVC. **NOTE: later it was decided to remove the factor of 9 from the post\_inversion software. Hence, the QC threshold table should now be computed as  $18.45 / (\text{MLE norm from step 2})$ .**

## Glossary

ASCAT	- Advanced SCATterometer
AWDP	- ASCAT Wind Data Processor
ECMWF	- European Centre for Medium-range Weather Forecast
ERS	- European Remote-Sensing satellite
GMF	- Geophysical Model Function
MLE	- Maximum Likelihood Estimate
NOC	- NWP-based OC
NWP	- Numerical Weather Prediction
OC	- Ocean Calibration
PDF	- Probability Distribution Function
SAF	- Satellite Application Facility
SD	- Standard Deviation
VOC	- Visual correction method for OC
WVC	- Wind Vector Cell
QC	- Quality Control

## References

[ASCAT user manual] A. Verhoef and A. Stoffelen, ASCAT Wind Product User Manual version 1.8, SAF/OSI/CDOP/KNMI/TEC/MA/126, EUMETSAT, 2010.

[EUMETSAT 2005] "ASCAT Product Generation Function Specification", EUM.EPS.SYS.SPE.990009, Issue 6 rev 6, Darmstadt Germany, April 11, 2005

[Freilich 1999] M. Freilich, H. Qi, and R. S. Dunbar, "Scatterometer beam balancing using open-ocean backscatter measurements," J. Atmos. Ocean. Technol., vol. 16, no. 2, pp. 283–297, Feb. 1999.

[NWPSAF site]  
<http://research.metoffice.gov.uk/research/interproj/nwpsaf/>

[KNMI site]  
[http://www.knmi.nl/scatterometer/ascat\\_osi\\_25\\_prod/ascat\\_app.cgi?cmd=buoy\\_validations](http://www.knmi.nl/scatterometer/ascat_osi_25_prod/ascat_app.cgi?cmd=buoy_validations)

[Stoffelen and Anderson 1997] Stoffelen, Ad, and Anderson, David, "Scatterometer Data Interpretation: Measurement Space and inversion", J. Atm. and Ocean Techn., 14(6), 1298-1313, 1997.

[Stoffelen 1998] Stoffelen, Ad, "Scatterometry", KNMI, *PhD thesis at the University of Utrecht*, ISBN 90-39301708-9, October 1998

[Verspeek 2006] Verspeek, Jeroen, "Scatterometer calibration tool development", EUMETSAT Technical Report SAF/OSI/KNMI/TEC/RP/092, KNMI, de Bilt, 2006

[Verspeek 2008] Jeroen Verspeek, Marcos Portabella, Ad Stoffelen, Anton Verhoef, Calibration and Validation of ASCAT Winds, SAF/OSI/KNMI/TEC/TN/163, KNMI, 2008.